

Design, Synthesis, and Biological Evaluation of Organic Nitrite (NO_2^-) Donors as Potential Anticerebral Ischemia Agents

Jianbing Wu,[#] Wei Yin,[#] Zhangjian Huang,^{*} Yinqiu Zhang, Jian Jia, Huimin Cheng, Fenghua Kang, Kai Huang, Tao Sun, Jide Tian, Xiaojun Xu,^{*} and Yihua Zhang^{*}



Cite This: *J. Med. Chem.* 2021, 64, 10919–10933



Read Online

ACCESS |



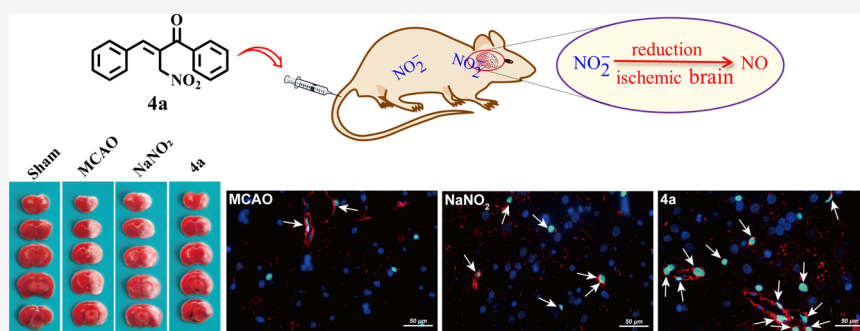
Metrics & More



Article Recommendations



Supporting Information



► **4a** reduces rat cerebral infarct volume and promotes angiogenesis in cerebral ischemic penumbra.

ABSTRACT: The treatment of ischemic stroke (IS) remains a big challenge in clinics, and it is urgently needed to develop novel, safe, and effective medicines against IS. Here, we report the design, synthesis, and biological evaluation of organic NO_2^- donors as potential agents for the treatment of IS. The representative compound **4a** was able to slowly generate low concentrations of NO_2^- by reaction with a thiol-containing nucleophile, and the NO_2^- was selectively converted into NO under ischemic/hypoxia conditions to protect primary rat neurons from oxygen–glucose deprivation and recovery (OGD/R)-induced cytotoxicity by enhancing the Nrf2 signaling and activating the NO/cGMP/PKG pathway. Treatment with **4a** at 2 h before or after ischemia mitigated the ischemia/reperfusion-induced brain injury in middle cerebral artery occlusion (MCAO) rats by producing NO and enhancing Nrf2 signaling. Furthermore, **4a** significantly promoted endothelial cell proliferation and angiogenesis within the ischemic penumbra. Our findings suggest that this type of NO_2^- donors, like **4a**, may be valuable to fight IS and other ischemic diseases.

INTRODUCTION

Ischemic stroke (IS) is a disease with a high mortality and morbidity, leading to a heavy socioeconomic burden globally. Although the intervention of IS has been advanced in the past decades, there is a lack of safe and effective treatments for this fatal disease.¹ Endovascular thrombectomy has shown great value for the treatment of acute IS (AIS). However, few stroke patients actually have received this treatment, and less than half of those with the treatment will benefit permanently.² Tissue plasminogen activator (tPA) is the only anti-AIS specific medicine approved by the Food and Drug Administration (FDA). Unfortunately, the very narrow time window and the potential risk of intracerebral hemorrhage of tPA greatly limit its wider clinical applications.³ Therefore, it is urgently needed to develop novel, safer, and more effective drugs against IS.

It is well established that surrounding the core of cerebral infarction in an AIS patient, there is a hypoxic area, named “ischemic penumbra”, which is sensitive to secondary injury and can be rescued by improving the blood flow to protect neurons from ischemic damage.⁴ Given that microvessel

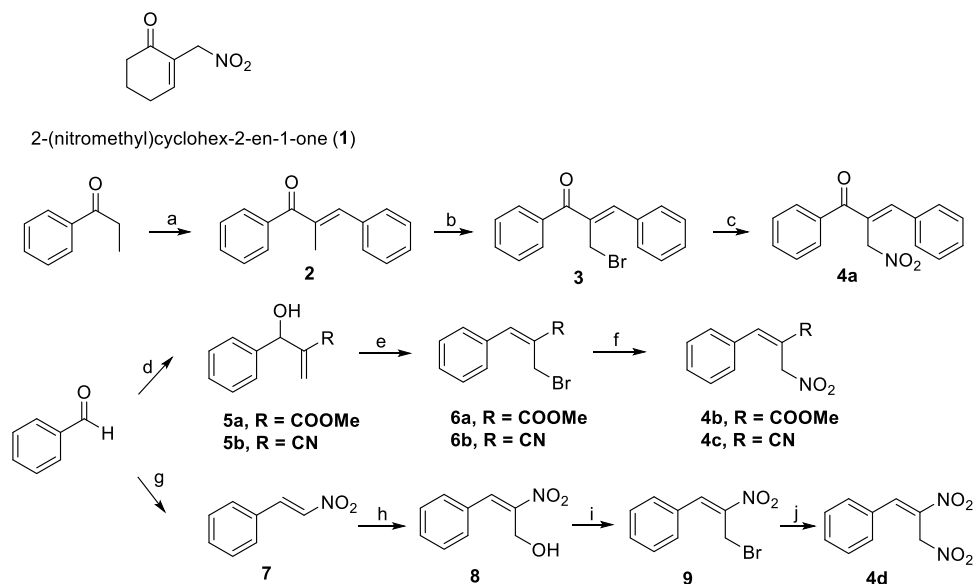
density is crucial for the survival of patients,⁵ the enhancement of therapeutic angiogenesis has become an attractive strategy for development of anti-IS drugs.

Nitric oxide (NO) is one of the most appealing gaseous molecules in the field of biomedical sciences. It functions as a key mediator in a wide range of biological events, including improving blood flow by inducing vessel dilation and promoting endothelial cells to form microvasculature. Moreover, NO can protect tissues against ischemic damage by reducing the process of cellular respiration.⁶ However, vascular NO bioavailability is reduced in ischemic tissues.^{7–9} Fortunately, the exogenous administration of NO donors can enhance angiogenesis in ischemic tissues and protect from

Received: February 14, 2021

Published: July 22, 2021



Scheme 1. Synthetic Route of Target Compounds 4a–d^a

^aReagents and conditions: (a) benzaldehyde, NaOH, ethanol, 70 °C, 12 h; (b) NBS, AIBN, CCl₄, reflux, 10 h; (c) AgNO₂, diethyl ether, r.t., overnight; (d) methyl acrylate or acrylonitrile, DABCO, r.t., 7–10 days; (e) PBr₃, CH₂Cl₂, 0 °C–r.t., 15 min; (f) AgNO₂, diethyl ether, r.t., overnight; (g) nitromethane, ammonium acetate, 100 °C, 8 h; (h) formaldehyde, imidazole, THF, r.t., 72 h; (i) PBr₃, CH₂Cl₂, 0 °C–r.t., 15 min; and (j) AgNO₂, diethyl ether, r.t., overnight.

ischemia injury.^{10,11} Nevertheless, the therapeutic effects of NO donors are both dose- and microenvironment context-dependent. It is well known that high concentrations of NO may cause cytotoxicity, impeding the utilities of NO donor-based therapy for ischemic diseases.¹² We hypothesize that it may be a safe and effective strategy to develop a NO donor that generates a relatively low amount of NO specifically in the ischemic region for the treatment of ischemic injury.

Interestingly, nitrite can be converted into NO through an enzyme-dependent or -independent manner in the ischemic region.^{13–15} In the ischemic regions, due to the lower pH and NO bioavailability, nitrite anion (NO₂⁻) can be reduced to NO by deoxygenated hemoglobin (deoxy-Hb), xanthine oxidoreductase (XOR), aldehyde oxidase, and others to promote vessel dilation and blood supply.¹⁶ In contrast, NO₂⁻ is usually oxidized into nitrate (NO₃⁻) in normoxic tissues and excreted in the urine.¹⁷ Thus, NO₂⁻ acts as a prodrug, which can be selectively converted into NO in the ischemic tissues to exert its beneficial effects.

Several sodium nitrite (NaNO₂)-based therapies have exhibited promising efficacy for the treatment of ischemic disorders in rodents.^{18–21} For example, the early intravenous administration of NaNO₂ reduced infarction volumes and improved cerebral blood flow and functional recovery to mitigate brain injury in a rat model of ischemia/reperfusion (I/R) injury.²² In the murine hindlimb ischemia model, a low dose of NaNO₂ significantly restored ischemic hindlimb blood flow, increased ischemic limb vascular density, and stimulated endothelial cell proliferation in a time-dependent manner.¹⁸ In addition, NaNO₂ at lower doses also exerts excellent cytoprotective effects in mouse models of I/R heart, liver, or kidney injury.^{20,21} Importantly, treatment with NaNO₂ benefits AIS patients and displays relatively high safety.¹⁹

However, as an inorganic salt, NaNO₂ is easily absorbed and rapidly metabolized after oral or intravenous administration, making the *in vivo* NO₂⁻ levels difficult to be accurately

controlled. Additionally, high doses of NaNO₂ failed to generate the desirable protective effects *in vivo*.^{18,22} Probably, the high levels of NO₂⁻ produce a massive amount of NO that subsequently generates high levels of the stronger oxidant peroxynitrite, leading to protein nitration, DNA damage, and energy failure.¹² Hence, the discovery of organic NO₂⁻ donors that release NO₂⁻ in a controlled and sustained manner for the treatment of ischemic diseases will be of great interest.

Currently, there are few reported NO₂⁻ donors except for allylic nitro compounds, exemplified by 2-(nitromethyl)cyclohex-2-en-1-one (**1**, Scheme 1), which was synthesized by King's group in 2006.²³ However, the pharmacological effects of these compounds were not disclosed, and actually, this type of donors released NO₂⁻ too fast to be controlled (see our data below).

Chalcone or (*E*)-1,3-diphenyl-2-propene-1-one is a common simple scaffold found in many naturally occurring compounds.²⁴ Chalcone derivatives and analogues have shown many interesting biological activities, including the antioxidant activity by activation of the nuclear factor (erythroid-derived 2)-like 2 (Nrf2) pathway, which is critical for mitigating the I/R-induced tissue damage in experimental ischemic stroke.^{25,26}

Since the NO₂⁻ release of compound **1** is too fast, which may be due to its high rigidity in structure resulting in the insufficient stability, in this study, we designed and synthesized compound **4a** by replacing the cyclohexenone structure with chain-like acrylketone, which was incorporated with a chalcone scaffold. Subsequently, we designed and synthesized a series of analogues of **4a** using other common unsaturated structures (carboxylate, cyano, and nitro groups, respectively) to replace the carbonyl in **4a**, and each of them linked to one nitromethyl group, like compound **1** as a NO₂⁻ donating moiety. Furthermore, we investigated their stability and NO₂⁻ releasing as well as evaluated their anti-ischemic effects *in vitro* and *in vivo*. Compound **4a** was one representative compound shown in Figure 1.

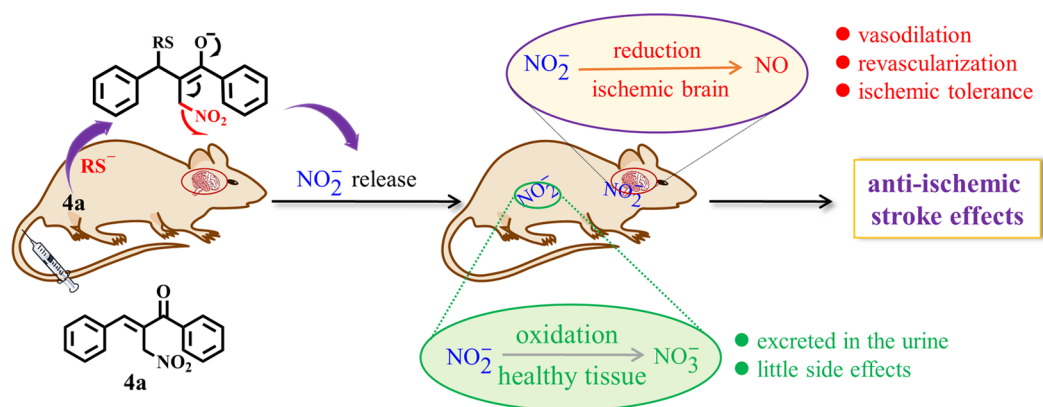


Figure 1. The rational design of NO_2^- donor (4a) and its potential NO -dependent action.

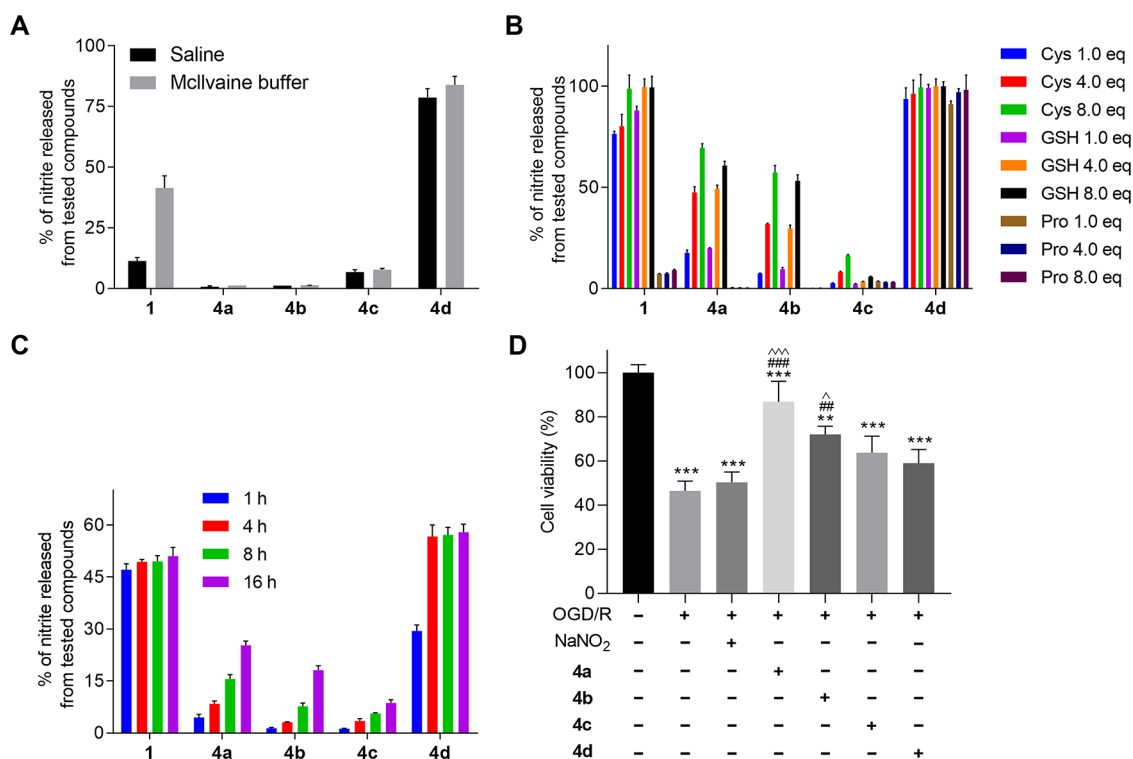


Figure 2. NO_2^- releasing behavior and neuronal protecting effects of NO_2^- donors. The levels of NO_2^- released (indicated as % of NO_2^- released from tested compounds, $200 \mu\text{M}$) from 1 and 4a–d (A) in saline and McIlvaine buffer; (B) in the presence of cysteine, glutathione, or proline; and (C) in bovine plasma. Data are expressed as the mean \pm SD of each group from three separate experiments. (D) The effect of indicated compounds on cell viability of primarily cultured rat neurons following OGD/R damage from three separate experiments. *** $P < 0.001$ vs the control group; ## $P < 0.01$, ### $P < 0.001$ vs the OGD/R group; ^ $P < 0.05$, ^^ $P < 0.001$ vs the NaNO_2 group.

RESULTS

Chemistry. The synthetic route of the target compounds 4a–d and their structures are depicted in Scheme 1. Starting from the aldol condensation of propiophenone with benzaldehyde, the resulting intermediate 2 was brominated using NBS and AIBN to give allyl bromide compound 3. The subsequent nitration of 3 using silver nitrite offered 4a. The treatment of benzaldehyde with methyl acrylate or acrylonitrile in the presence of 1,4-diaza[2.2.2]bicyclooctane (DABCO) produced allyl alcohol compounds 5a and 5b, respectively. Bromination of 5a and 5b with phosphorus tribromide generated allyl bromide compounds 6a and 6b. The nitration of 6a and 6b with silver nitrite away from light furnished target compounds 4b and 4c, respectively. On the other hand, in the

presence of a catalytic amount of ammonium acetate, benzaldehyde reacted with nitromethane to form the mononitro compound 7. Treatment of 7 with formaldehyde catalyzed by imidazole provided nitro allyl alcohol 8, which was brominated by phosphorus tribromide to give bromide intermediate 9. The target compound 4d was finally obtained by the reaction of 9 with silver nitrite in the dark.²⁷

4a–d Release NO_2^- under Various Conditions. Given that an ideal organic NO_2^- donor compound should slowly release NO_2^- by a given trigger, we next examined and compared the levels of NO_2^- released from NO_2^- donor 1 and 4a–d under various conditions (Figure 2). The relationship between the structures and NO_2^- releasing behaviors of these target compounds revealed that after incubation in physiological saline or McIlvaine buffer, 1 and 4d with two nitro

groups in their structure released relatively high levels of NO_2^- , while **4a–c** each with one nitro group failed to release or released very low levels of NO_2^- (Figure 2A), suggesting that the target compounds **4a–c** may be more stable than both **1** and **4d** in physiological conditions. To examine whether the target compounds could be activated by exogenous nucleophiles to release NO_2^- , we incubated each compound with cysteine (Cys), glutathione (GSH), or proline (Pro) for 1 h and measured the levels of NO_2^- (Figure 2B). Compounds **1** and **4d** released approximately 99% of their theoretical levels of NO_2^- (except for **1** in the presence of Pro). In contrast, **4c** released very low levels of NO_2^- in the presence of these three nucleophiles. Interestingly, **4a** and **4b** released moderate levels of NO_2^- in the presence of GSH or Cys in a concentration-dependent manner but did not release detectable NO_2^- in the presence of Pro, indicating that **4a** and **4b** were only activated by thiol-containing nucleophiles. In addition, we observed that **1** and **4d** rapidly released NO_2^- , while **4a–c** slowly released lower levels of NO_2^- in bovine plasma (Figure 2C).

4a–d Protect from the OGD/R-Induced Neuronal Injury. Next, we examined the activity of all target compounds on their neuroprotective effects. Briefly, primary rat neurons were treated with NaNO_2 and **4a–d** (1.8 μM each) for 24 h and subjected to OGD for 2 h followed by culture in normoxic conditions for 24 h. The cell viability of each group of cells was tested (Figure 2D). The relationship between the structures and neuroprotective effects of the target compounds indicated that **4a** with both the NO_2^- releasing group and the chalcone scaffold remarkably reduced the OGD/R-induced damage in primarily cultured neurons, superior to NaNO_2 and all other target compounds, probably because **4a** slowly released moderate levels of NO_2^- . The compounds **4b** and **4c** had only one NO_2^- releasing group as well as one carboxylate or cyano group in their structures and displayed neuroprotective activities weaker than **4a**, which may stem from the relatively lower levels of NO_2^- released by **4b** and **4c** than that by **4a**. And **4b** had a slightly stronger neuroprotective activity than **4c**, which may also be due to **4b** releasing somewhat larger amounts of NO_2^- than **4c**. Additionally, **4d** with two nitro groups in its structure displayed moderate levels of neuroprotective activity, which may be due to its high NO_2^- releasing rate, leading to the generation of a massive amount of NO toxic to neurons. Based on these results, we chose **4a** as the representative compound for the following experiments.

Examination of 4a Stability. The stability of **4a** in the presence of light, in PBS solutions at different pHs, and in rat plasma was examined (Figure S1, Supporting Information). We found that **4a** had similar stability in the presence or absence of light with almost no change during a 24 h observation period, and **4a** was relatively stable at pH 7.4 in saline and in rat plasma with a half-life period ($t_{1/2}$) of 38.5 and 5.3 h, respectively, but relatively unstable at pH 6 ($t_{1/2} = 1.1$ h). Additionally, the reaction rate of **4a** with GSH was positively correlated with the levels of GSH (Figure S2, Supporting Information), and the reaction rate constant K for 1, 4, 8, and 32 equiv of GSH was calculated as 0.0214, 0.0299, 0.0363, and 0.0560 h^{-1} , respectively.

4a Releases NO_2^- In Vivo. Before the *in vitro* and *in vivo* biological evaluation, the physicochemical property of **4a** was examined. We found that **4a** had a water solubility of 33.21 ± 3.49 mg/L (124.38 ± 13.06 $\mu\text{mol/L}$, 37 $^\circ\text{C}$) and a lipo-hydro partition coefficient $\log P$ of 0.54 ± 0.025 . We then tested the ability of **4a** to release NO_2^- and the PK behavior of **4a** *in vivo*.

Briefly, male Sprague–Dawley (SD) rats were injected iv with an equimolar **4a** (10 mg/kg) or NaNO_2 (2.44 mg/kg). The blood concentrations of **4a** and NO_2^- were quantified at 2, 5, 15, 30, 60, 90, and 120 min post injection by LC–MS/MS and ion chromatography,²⁴ respectively. The results were shown in Figure 3, Figure S3 (Supporting Information), and Table S1

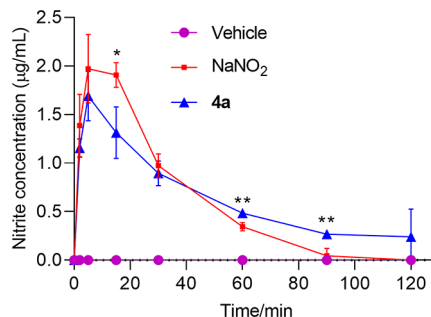


Figure 3. *In vivo* determination of NO_2^- released by **4a**. The concentrations of orbital blood NO_2^- in rats were tested at 2, 5, 15, 30, 60, 90, and 120 min post iv administration of **4a** (10 mg/kg) or NaNO_2 (2.44 mg/kg), respectively. Data are presented as means \pm SD of each group ($n = 3$ per group) of rats. * $P < 0.05$, ** $P < 0.01$ vs the NaNO_2 group at the indicated time points.

(Supporting Information). We found that the administration of NaNO_2 induced a rapid increase in the blood concentrations of NO_2^- with a peak at 5–15 min and a gradual decrease to the basal level at 90 min. In contrast, treatment with **4a** significantly reduced the peak blood NO_2^- concentrations but maintained lower levels of blood NO_2^- until 120 min post injection (the longest time point for analysis). These results indicated that **4a** produced moderate levels of NO_2^- *in vivo* for a longer period relative to NaNO_2 , which may be beneficial for the treatment of ischemia.

Mechanism Study on NO_2^- Release from 4a. The ^1H NMR technique was used for the first time to study the possible mechanism of NO_2^- release from **4a**, which was used alone or mixed with 1.5 equiv of *N*-acetyl Cys for 5, 30, 60, 120, and 600 min in anhydrous d_6 -DMSO at 37 $^\circ\text{C}$ (Figure 4). As shown in Figure 4A–D, following the addition of *N*-acetyl Cys to the **4a** solution, mono-SR intermediate **10** was formed by a rapid thio-addition and nitro-elimination sequence with the characteristic signals for H_a ($\delta = 5.3$, $J = 6$ Hz) and for H_b and H_c ($\delta = 6.2$ and 5.8, $J = 9$ Hz) as well as for H_d ($\delta = 3.9$, the proton adjacent to the NHAc group in *N*-acetyl Cys). The double bond of **10** was then gradually converted to a single bond, and the signals for H_b and H_c were shifted to high field and overlapped in the signal peaks for *N*-acetyl Cys (Figure 4E,F), suggesting that another molecule of *N*-acetyl Cys may attack the double bond at the β -position of **10** to form an intermediate, which is rapidly converted to di-SR compound **12**.

Another alternative route of NO_2^- release might result from a direct $\text{S}_{\text{N}}2$ nucleophilic substitution of the nitro group in **4a** by *N*-acetyl Cys, which produced mono-SR intermediate **11** with a signal of H_d' ($\delta = 3.8$). However, **11** might further undergo thio-addition reaction to generate di-SR compound **12**.

Because the polarity of each intermediate was substantially increased after reaction with thiols, it was very difficult to separate or purify these unstable intermediates. Fortunately, however, we identified the molecular weights of these intermediates using LC–HRMS (see Supporting Information).

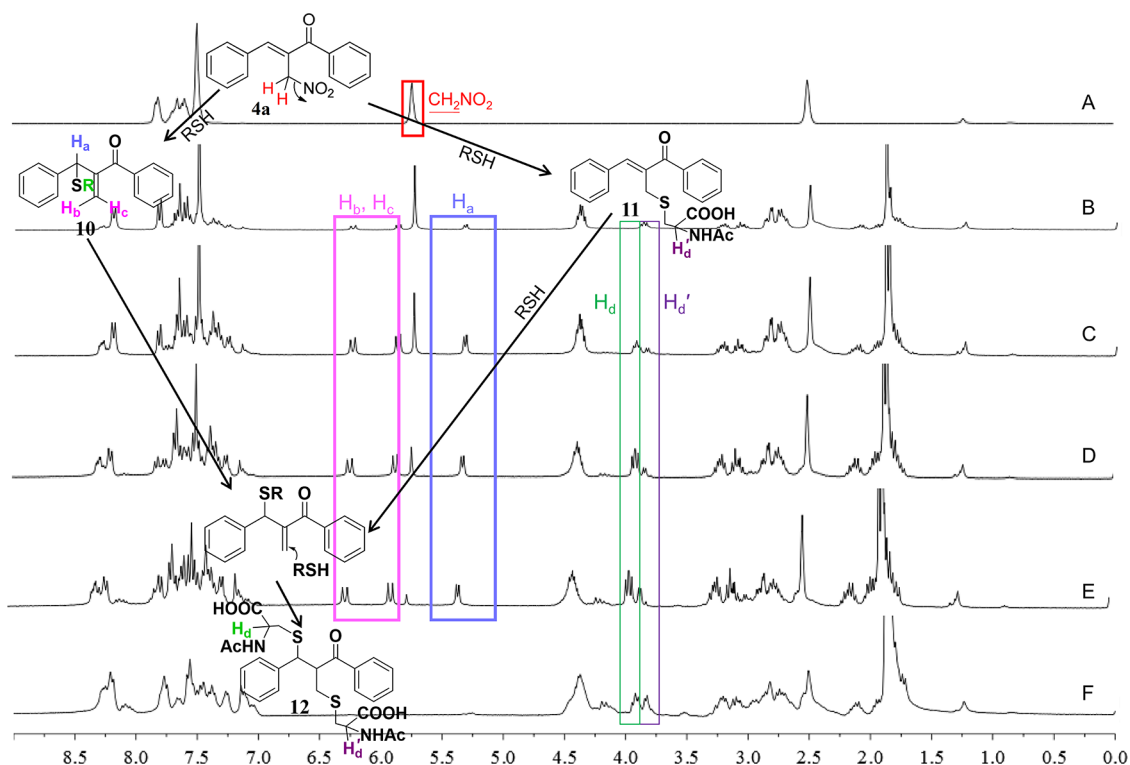


Figure 4. ^1H NMR spectra of **4a** (40 mM) in anhydrous d_6 -DMSO at 37°C . (A) **4a** was used alone. (B–F) **4a** was mixed with *N*-acetyl Cys (60 mM) for 5, 30, 60, 120, and 600 min, respectively.

The presence of intermediates formed by the reaction of compound **4a** with one and/or two GSH/*N*-acetyl Cys could be preliminarily identified by HRMS from their molecular weights of 527/383 and 834/546, respectively. These data may support our above mechanistic study on NO_2^- release from chalcone **4a**.

4a Protects from the OGD/R-Induced Neuronal Injury. 4a Enhances the Nrf2 Signaling. Given that **4a–d** bearing a chalcone scaffold can serve as a potential Michael acceptor, it may biologically form a covalent bond with the sulfhydryl of cysteine in proteins, displaying pharmacological activities. It is notable that chalcones can activate the Kelch-like ECH-associated protein 1 (Keap1)/Nrf2/ARE pathway through the covalent modification of the cysteines of Keap1 to release Nrf2, inducing the expression of phase II enzymes and antioxidant enzymes that protect from the oxidative-stress-induced I/R injury.²⁸ Accordingly, the neuroprotective effect of the **4a** was first examined and compared with NaNO_2 , and a Nrf2 activator, *tert*-butylhydroquinone (TBHQ). Primary rat cortical neurons were isolated and pretreated with **4a**, NaNO_2 , or TBHQ at the optimized concentration of $1.8\ \mu\text{M}$ for 24 h and subjected to OGD for 2 h followed by culture in normoglycemic and normoxic conditions for 24 h. The apoptosis rate, cell viability, and lactate dehydrogenase (LDH) activity in the supernatants of cultured cells were tested. In comparison with the control, the OGD/R significantly increased the percentages of apoptotic cells (Figure 5A,B) and LDH activities (Figure 5C) but significantly reduced the cell viability (Figure 5D) in the cultured primary rat neurons *in vitro* ($P < 0.001$ for all). Treatment with NaNO_2 mitigated the OGD/R-increased LDH activity ($P < 0.01$) but did not significantly alter cell apoptosis and viability in the neurons following OGD/R. In contrast, treatment with **4a**, like

TBHQ, remarkably reduced the OGD/R-mediated cytotoxicity in the cultured primary rat neurons, which was mitigated by the treatment with a Nrf2 inhibitor, ML385 ($5\ \mu\text{M}$)^{29,30} (Figure S4, Supporting Information). These results indicated that **4a** had potent neuroprotective activity against the OGD/R-induced neuronal injury, at least partially, by enhancing the Nrf2 signaling.

Next, to determine whether **4a** may activate the Keap1/Nrf2 signaling, rat primary cortical neurons were treated with or without **4a** ($1.8\ \mu\text{M}$), NaNO_2 ($1.8\ \mu\text{M}$), or TBHQ ($1.8\ \mu\text{M}$) for 24 h and subjected to OGD/R. The relative levels of Nrf2, HO-1, and NQO1 mRNA transcripts were determined by RT-qPCR, and cytoplasmic and nuclear Nrf2 protein levels were evaluated by Western blot analysis. In comparison with the control, the OGD/R or pretreatment with any of the compounds did not significantly alter the relative levels of Nrf2 mRNA transcripts (Figure 5E). Furthermore, while the OGD/R significantly reduced the relative ratios of nuclear to cytoplasmic Nrf2 protein (Figure 5F–H), pretreatment with **4a**, and compound **2** (with the chalcone backbone of **4a** but without the nitro group) or TBHQ, but not NaNO_2 , significantly mitigated the effect of OGD/R by increasing the relative ratios of nuclear to cytoplasmic Nrf2 protein ($P < 0.001$), indicating that **4a** enhanced the Nrf2 signaling by promoting its nuclear translocation in the primary rat neurons following OGD/R. Consequently, pretreatment with **4a** or TBHQ significantly mitigated the OGD/R-decreased HO-1 and NQO1 (target genes of Nrf2) mRNA transcription in primary rat neurons (Figure 5I,J). These data further evidenced that **4a** protected the primary rat neurons from the OGD/R-induced neuronal injury by enhancing the Nrf2 signaling *in vitro*.

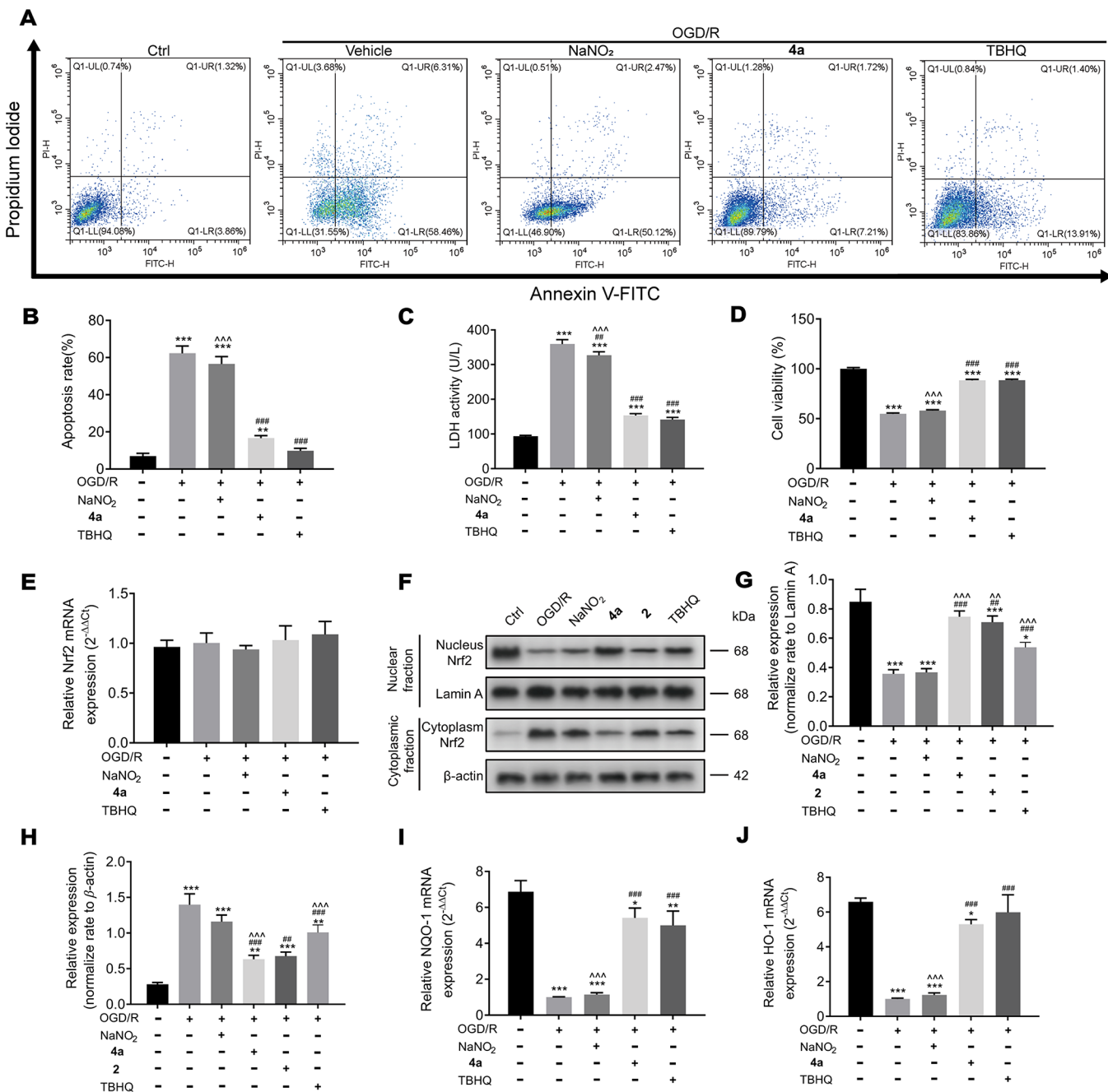


Figure 5. 4a protects from the OGD/R-induced neuronal injury by enhancing the Nrf2 signaling. (A and B) Flow cytometry analysis of the frequency of apoptotic cells. (C) LDH activity. (D) MTT analysis of cell viability. (E) RT-qPCR analysis of the relative levels of Nrf2 mRNA transcripts. (F–H) Western blot analysis of nuclear and cytoplasmic Nrf2 protein. (I and J) RT-qPCR analysis of the relative levels of NQO-1 and HO-1 mRNA transcripts. Data are representative images or expressed as the mean \pm SD of each group of cells from three independent experiments. * $P < 0.05$, ** $P < 0.01$, *** $P < 0.001$ vs the control group; ### $P < 0.01$, #### $P < 0.001$ vs the OGD/R group; ^^ $P < 0.001$ vs the NaNO₂ group.

4a Activates the NO/cGMP/PKG Pathway. Additionally, we examined whether 4a functioned *via* the NO₂⁻/NO/cGMP/PKG pathway in primary rat neurons. The results showed that 4a protected neurons from the OGD/R-induced injury and increased the levels of cGMP and PKG2 expression in the primarily cultured neurons under OGD/R as compared to those in the untreated control. Importantly, most of the effects of 4a were abrogated by treatment with a known sGC inhibitor, NS2028 (Figure S5, Supporting Information).

Pretreatment with 4a Protects from the I/R-Induced Brain Injury in MCAO Rats. Next, we tested whether

pretreatment with 4a could protect from the I/R-induced brain injury in rats. The different groups of rats were injected iv with the indicated compounds through their tail vein. Two hours later, they were subjected to middle cerebral artery occlusion (MCAO) for 2 h followed by reperfusion. One day post the I/R procedure, their neurologic deficits were scored and their brain tissue ischemic volumes and cerebral edema degrees were evaluated in a blinded manner. As shown in Figure 6, treatment with different doses of NaNO₂ did not significantly alter the brain infarct volumes, cerebral edema degrees, or neurologic deficit scores in rats relative to those in the vehicle-

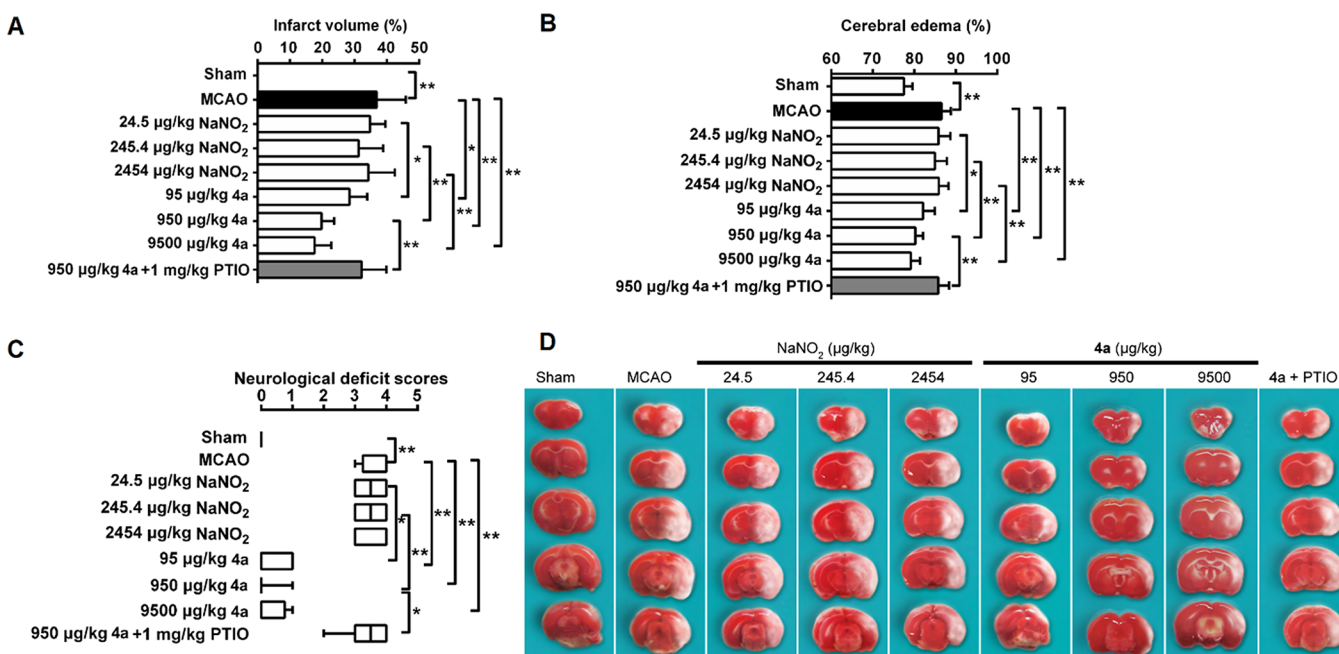


Figure 6. Pretreatment with 4a protects rats from cerebral I/R injury. Rats were treated iv with the vehicle saline, NaNO_2 , 4a, or 4a + PTIO, and 2 h later, the rats were subjected to the MCAO procedure. At 24 h post I/R procedure, the rats were scored for their neurological deficits. Subsequently, the rats were euthanized and their brain tissues were stained by TTC. (A) Infarction volumes (%) were calculated as infarct area/whole area for each group. (B) Cerebral edema (%) was calculated by the formula illustrated in the method section. (C) The neurological deficit scores were analyzed by the Kruskal–Wallis test followed by the Mann–Whitney U test for multiple comparisons. (D) The representative images of brain sections in each group after TTC staining. Data are presented as mean \pm SD or median \pm IQR of each group ($n = 8$). * $P < 0.05$, ** $P < 0.01$.

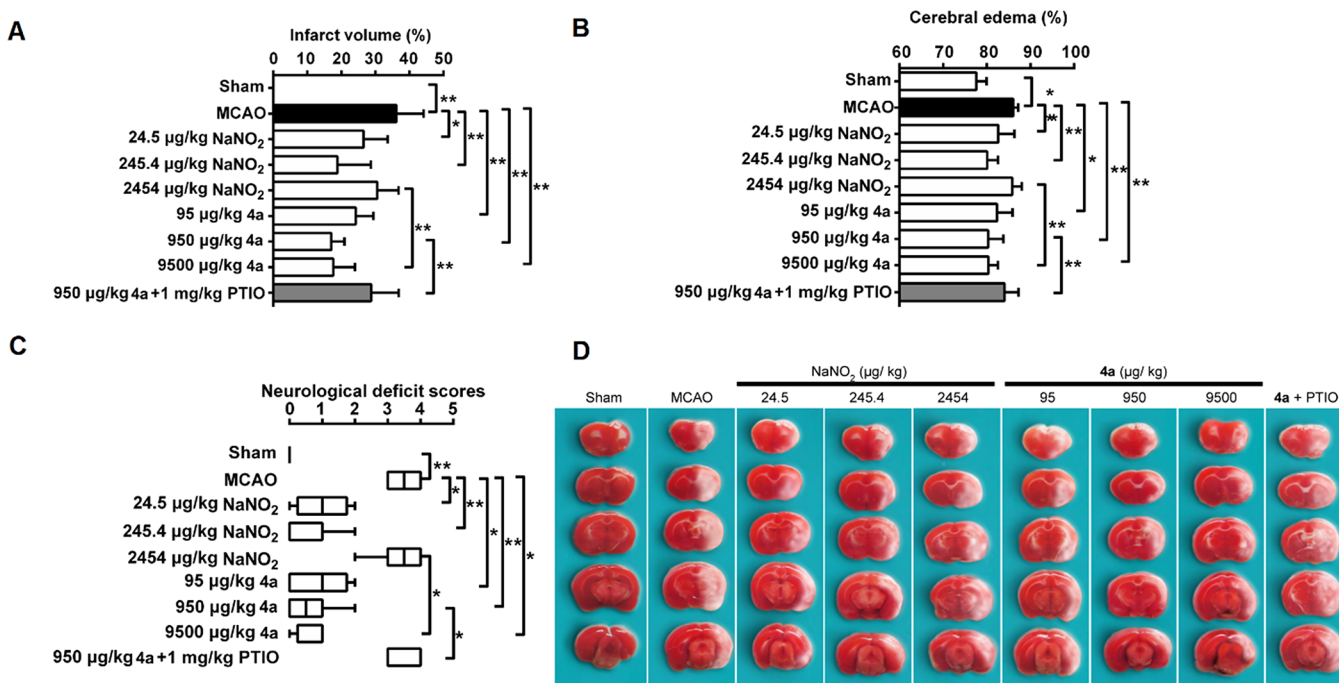


Figure 7. Treatment with 4a after MCAO reduces the cerebral I/R injury in rats. Two hours after MCAO, the rats were randomized and treated iv with the vehicle (as the MCAO group), NaNO_2 , 4a, or 4a + PTIO immediately after perfusion. At 24 h post I/R, their neurological deficits were scored and their brain sections were stained by TTC. (A) Infarction volumes (%) were calculated as infarct area/whole area for each rat. (B) Cerebral edema (%) was calculated by the formula illustrated in the method section. (C) The neurological deficit scores were analyzed by the Kruskal–Wallis test followed by the Mann–Whitney U test for multiple comparisons. (D) The representative images of brain sections in each group after TTC staining. Data are presented as mean \pm SD or median \pm IQR of each group ($n = 8$). * $P < 0.05$, ** $P < 0.01$.

treated MCAO group. Treatment with different doses of 4a substantially reduced the brain infarct volumes, cerebral edema

degrees, and neurologic deficit scores in rats, and their protective effects appeared to be dose-dependent. Importantly,

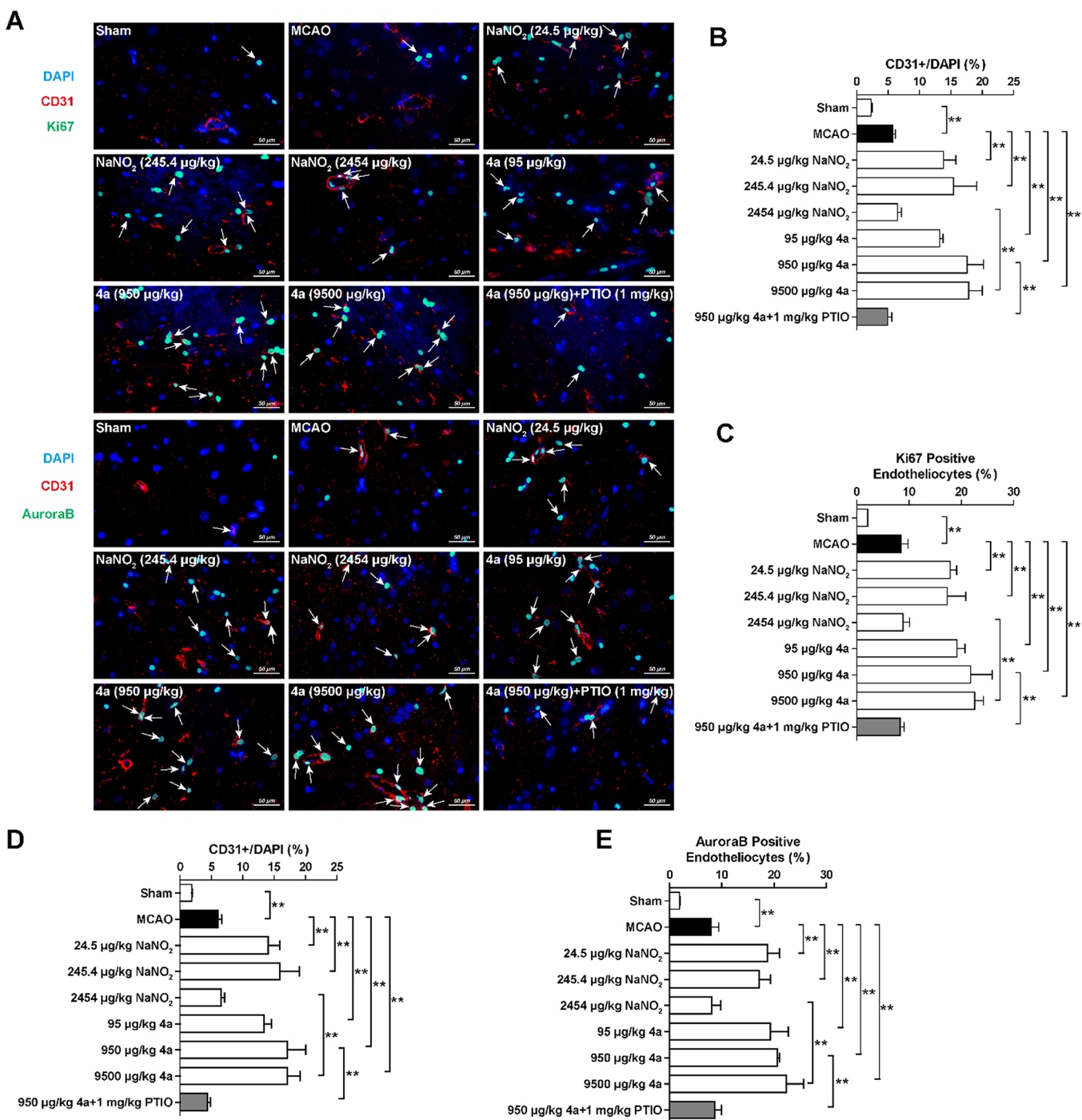


Figure 8. 4a promotes angiogenesis in rat cerebral ischemic penumbra. Following treatment with saline, the indicated doses of NaNO₂, or 4a for a week, the CD31 expression and Ki67⁺ and Aurora B⁺ cells were determined by IHC and immunofluorescent assays. (A) Representative images of anti-Ki67 (green), anti-Aurora B (green), anti-CD31 (red), and nuclear DAPI (blue) staining in the brain sections, respectively. (B and C) Quantitative analysis of the percentages of CD31⁺/DAPI⁺ and Ki67⁺/DAPI⁺ endothelial cells. (D and E) Quantitative analysis of the percentages of CD31⁺/DAPI⁺ and Aurora B⁺/DAPI⁺ endothelial cells. Scale bar, 50 μ m. Data were presented as mean \pm SD of each group ($N = 5$). * $P < 0.05$, ** $P < 0.01$.

treatment with 4a, together with a NO scavenger, PTIO (2-phenyl-4, 4, 5, 5-tetramethylimidazoline-1-oxyl 3-oxide, 1 mg/kg), almost abolished the therapeutic effect of 4a in MCAO rats. Together, these results indicated that pretreatment with 4a significantly prevented the I/R-mediated brain injury in rats predominantly by producing NO.

In addition, we observed that iv injection with 4a (950 μ g/kg) displayed little effect on the systemic blood pressure during

a 24 h observation period (Figure S6, Supporting Information). This may be because 4a, as an organic NO₂⁻ donor, would not release high levels of NO directly in the blood circulation. Instead, 4a sustainably released moderate levels of NO₂⁻ that was converted into low levels of NO under the hypoxic conditions in ischemic regions. Therefore, NO₂⁻ donating compounds, like 4a, may not significantly alter systemic blood pressure.

Treatment with 4a after I/R Reduces the Cerebral I/R Brain Injury in MCAO Rats.

To investigate the therapeutic effects of **4a** on the I/R-induced brain damage in rats, male SD rats were subjected to MCAO for 2 h followed by blood reperfusion. The rats were randomized and injected iv with the vehicle, **4a**, NaNO₂, or **4a** + PTIO at the indicated doses immediately after reperfusion. A group of rats received a sham procedure (the sham group) and was injected iv with the vehicle. The brain infarct volumes, cerebral edema degrees, and neurologic deficit scores in all rats were evaluated in a blinded manner at 24 h post I/R procedure (Figure 7). The MCAO group of rats displayed severe brain tissue infarction, higher degrees of brain edema, and higher neurologic deficit scores. Treatment with NaNO₂ at 24.5 or 245.4 μg/kg significantly reduced the brain infarct volumes, cerebral edema degrees, and neurologic deficit scores with a trend of dose-dependence ($P < 0.05$ or $P < 0.01$ for all). However, treatment with a higher dose of NaNO₂ only generated a minor reduction in the brain infarct volumes. In contrast, treatment with low and medium doses of **4a** significantly decreased the brain infarct volumes, cerebral edema degrees, and neurologic deficit scores ($P < 0.01$ and $P < 0.05$). The therapeutic effect of **4a** at the high dose was similar to that of its medium dose. Importantly, PTIO (1 mg/kg) almost abrogated the therapeutic effects of **4a** on the MCAO-mediated brain injury in rats. These data indicated that **4a** treatment reduced the MCAO-induced brain damages in rats predominantly by producing NO.

4a Enhances the Keap1/Nrf2/ARE Signaling in Rat Cerebral Ischemic Penumbra. Given that **4a** effectively enhanced the Nrf2 signaling to induce its target gene expression in the cultured primary rat neurons following OGD/R, we tested whether treatment with **4a** could also enhance the Nrf2 signaling by increasing its phosphorylation and target gene expression in rat ischemic brains by immunohistochemistry. First, phosphorylated Nrf2 signals were detected predominantly in the nuclei, while NQO-1 and HO-1 signals were observed mainly in the cytoplasm of cells (Figure S7A, Supporting Information). Quantitative analysis indicated that the I/R process significantly enhanced the Nrf2 phosphorylation and NQO-1 and HO-1 expression in rat cerebral ischemic penumbra (Figure S7B, Supporting Information). Treatment with **4a**, but not NaNO₂, significantly further increased the relative levels of Nrf2 phosphorylation and NQO1 and HO-1 expression in rat ischemic brain regions, suggesting that **4a** treatment may enhance the Nrf2 activation in the ischemic penumbra of rat brains.

4a Promotes Angiogenesis In Vitro and in Rat Cerebral Ischemic Penumbra. Enhancement of angiogenesis is crucial for the restoration of blood flow in the ischemic penumbra and closely correlated with the prognosis of cerebral stroke.³¹ Given that the activation of the Nrf2 signaling and its target HO-1 expression promote angiogenesis following the I/R induction,^{32–34} we evaluated the effects of **4a**, NaNO₂, compound **2**, and the combination of NaNO₂ and **2** on angiogenesis by using a commercial angiogenesis tube formation assay kit. As shown in Figure S8 (Supporting Information), treatment with **4a** (1.8 μM), with the same dose as NaNO₂, remarkably promoted tube formation in HUVECs, and the effect of **4a** on tube formation was significantly diminished by treatment with a known sGC inhibitor, NS2028. Compound **2** exerted a weaker effect; however, the combination of NaNO₂ and **2** increased tube formation in HUVECs, suggesting that both NO₂⁻ releasing group and

chalcone scaffold in **4a** may synergistically enhance tube formation in HUVECs.

Furthermore, we tested whether continual treatment with **4a** for 7 days could enhance angiogenesis in rat cerebral ischemic penumbra by immunofluorescence. As shown in Figure 8, the I/R procedure significantly increased the CD31 expression and Ki67⁺ cell frequency relative to those of the sham group, reflecting compensative responses after I/R process. Treatment with a low or medium dose of NaNO₂, but not a high dose of NaNO₂, significantly increased the CD31 expression and the percentages of Ki67⁺ cells or Aurora B⁺ cells, particularly for those Ki67⁺ or Aurora B⁺ endothelial cells (double staining of anti-CD31 and anti-Ki67 or double staining of anti-CD31 and anti-Aurora B). More importantly, treatment with either dose of **4a**, like the low or moderate dose of NaNO₂, significantly enhanced the CD31 expression and increased the frequency of Ki67⁺ or Aurora B⁺ endothelial cells, which were almost abrogated by co-treatment with PTIO. These results suggest that treatment with **4a** after I/R may significantly enhance the I/R-related angiogenesis, mainly dependent on its NO production in rat cerebral ischemic penumbra.

DISCUSSION

NO can induce vasodilation and ischemic tolerance.³⁵ However, in an acute hypoxic status, NO levels are reduced due to decreased levels of NOS expression.¹⁷ Instead, a variety of molecules, including hemoglobin-associated globulin, molybdenum-containing enzymes, cytochrome P450, and others, recycle NO from NO₂⁻ in a hypoxic condition, providing an alternative pathway for NO production.^{15,36,37} A number of NaNO₂-based therapies have been reported to be promising for the treatment of IS in both animals and humans. Unfortunately, the enteral administration with NaNO₂ may have the potential issue of bioavailability,¹⁷ while the intravenous administration with NaNO₂ can cause its rapid metabolism. Accordingly, the *in vivo* process of NO₂⁻ is difficultly controlled, limiting its wider application.

In this study, we developed a group of chalcone derivative **4a** and its analogues **4b–d**, which acted as organic NO₂⁻ donors. We observed that **4a** and **4b** released moderate levels of NO₂⁻ in bovine plasma and in the presence of cysteine or glutathione but not proline. **4a** generated lower maximum concentrations of NO₂⁻ for a longer duration than NaNO₂ in rats. We employed the ¹H NMR technique for the first time to study the mechanism underlying thiol-induced NO₂⁻ release from **4a** and found that **4a** liberated NO₂⁻ by sequential thio-addition and nitro-elimination reaction mechanisms.

Additionally, in OGD/R primary cortical neurons and MCAO rats, **4a** enhanced the Nrf2 signaling to protect the cells and rat brains from I/R injury, which was superior to NaNO₂. The results suggest that the chalcone scaffold in **4a** may enhance the Nrf2 signaling partly through a Michael addition reaction of the sulfhydryl in Keap1 to release Nrf2 and subsequent phosphorylation in the neurons in rat ischemic lesions.²⁶ Meanwhile, the NO₂⁻ released from **4a** activated the NO/cGMP/PKG pathway. Thus, both Nrf2 enhancement and cGMP/PKG activation synergistically contributed to the neuroprotection effects of **4a**. More importantly, the NO scavenger PTIO almost abrogated the therapeutic effects of **4a** on the MCAO-mediated brain injury in rats, and a known sGC inhibitor, NS2028, eliminated most of the protection of **4a** from the OGD/R-induced injury, suggesting that **4a** may exert

its anti-ischemic activity mainly by activating the NO/cGMP/PKG pathway.

One of the promising therapeutic strategies for the treatment of I/R-related injury is to promote angiogenesis and ameliorate penumbra damage after I/R. Indeed, we did find that **4a** promoted angiogenesis *in vitro*, treatment of MCAO rats with **4a** promoted endothelial cell proliferation and stimulated angiogenesis within the ischemic penumbra of rats, and most of the effects of **4a** were abrogated by a NO scavenger, PTIO. These observations suggest that **4a** may slowly release moderate levels of NO₂⁻ that was subsequently converted into NO in hypoxic penumbra to protect and rescue neurons in ischemic lesions. More importantly, the preventive and therapeutic effects of **4a in vivo** suggest that **4a**-like NO₂⁻ donors may have a broad therapeutic window for intervention of I/R-related tissue injury in clinical applications. In addition, unlike NaNO₂, treatment with **4a** avoids the uptake of Na⁺ into the blood, which may reduce the risk of Na⁺-induced cardiovascular events.³⁸

CONCLUSIONS

In summary, **4a** was the first organic NO₂⁻ donor bearing a chalcone scaffold with significant preventive and therapeutic effects on protecting against I/R brain injury by producing NO, enhancing the Nrf2 signaling, activating the NO/cGMP/PKG pathway, and promoting angiogenesis in the ischemic penumbra of rats. Therefore, **4a** may be a valuable lead compound for the development of new therapeutic agents for the treatment of ischemic stroke. This type of organic NO₂⁻ donors may be beneficial and helpful to promote the NO₂⁻-based therapies against ischemic diseases, including ischemic stroke.

EXPERIMENTAL SECTION

General. ¹H NMR and ¹³C spectra were recorded with a BrukerAvance 300 MHz spectrometer at 303 K using TMS as an internal standard. MS spectra were recorded on a Mariner Mass Spectrum (ESI) and high-resolution mass spectrometry (HRMS) on an Agilent Technologies LC/MSD TOF. Analytical and preparative TLC was performed on silica gel (200–300 mesh) GF/UV 254 plates, and the chromatograms were visualized under UV light at 254 and 365 nm. The purity of all target compounds was determined by HPLC (Shimadzu LC-20A HPLC system consisting of LC-20AT pumps and an SPD-20AV UV detector), and the compounds with a purity of >95% were used for the following experiments (see HPLC traces in Supporting Information). All solvents were reagent grade and, when necessary, were purified and dried by standard methods. Solutions after reactions and extractions were concentrated using a rotary evaporator operating at a reduced pressure of ca. 20 Torr. Compounds **4a–4c**,^{39–41} **5a–5c**,^{39–41} **6**,⁴² **7**,⁴³ and **8**⁴⁴ were synthesized as previously described.

The Synthesis of (E)-2-Methyl-1,3-diphenylprop-2-en-1-one (2). To a stirred solution of propiophenone (10 mmol, 1.34 g) and benzaldehyde (0.224 g, 12 mmol, 1.27 g) in EtOH (20 mL) was added NaOH (0.8 g, 20 mmol). The mixture was heated to 70 °C and stirred for 12 h. The reaction mixture was acidified to pH 2 using aq 2 N HCl and extracted with ethyl acetate (20 mL × 3). The combined organic layers were dried using anhydrous sodium sulfate, concentrated, and purified by flash chromatography (petroleum ether/EtOAc, 20:1 v/v) to afford **2** (1.44 g, 65%) as a colorless oil.⁴⁵ ¹H NMR (300 MHz, CDCl₃): δ 7.72–7.78 (m, 2H), 7.51–7.58 (m, 1H), 7.31–7.50 (m, 7H), 7.18 (d, 1H, J = 1.4 Hz), 2.28 (d, 3H, J = 1.4 Hz); ¹³C NMR (75 MHz, CDCl₃): δ 199.2, 142.0, 138.4, 136.7, 135.6, 131.5, 129.6, 129.3, 128.5, 128.3, 128.1, 14.3.

The Synthesis of (Z)-2-(Bromomethyl)-1,3-diphenylprop-2-en-1-one (3). To a solution of **2** (444.2 mg, 2 mmol) and NBS

(427.2 mg, 2.4 mmol) in dry CCl₄ (10 mL) was added AIBN (32.8 mg, 0.2 mmol). The mixture was refluxed for 10 h under a nitrogen atmosphere. The resulting reaction mixture was cooled to room temperature and filtered, and the filtrate was concentrated under a reduced pressure. The resulting residue was extracted with ethyl acetate (10 mL) three times. The organic layer was separated and dried using anhydrous sodium sulfate, concentrated, and purified by flash chromatography (petroleum ether/EtOAc, 15:1 v/v) to afford **3** (492 mg, 82%) as a colorless oil. The NMR data were consistent with a previous report.⁴⁶

General Procedure for the Preparation of 5a–b. To a solution of benzaldehyde (1.06 g, 10.0 mmol, 1.0 equiv) and DABCO (1.12 g, 10.0 mmol, 1.0 equiv) in methanol (20 mL) was added the respective substituted ethylene (50 mmol, 5.0 equiv). The reaction mixture was allowed to stir at r.t. for 1–4 days. The mixture was diluted by EtOAc (100 mL), washed by water (50 mL × 3) and brine (50 mL × 3), dried by anhydrous sodium sulfate, concentrated under vacuum, and purified by flash chromatography (petroleum ether/EtOAc, 1:1 v/v) to get **5a–b**.

Methyl 2-(Hydroxy(phenyl)methyl)acrylate (5a). The title compound was prepared from the reaction of benzaldehyde with methyl acrylate as a colorless oil in a yield of 35%. ¹H NMR (300 MHz, CDCl₃): δ 7.15–7.64 (m, 5H), 6.32 (s, 1H), 5.81 (s, 1H), 5.54 (s, 1H), 3.70 (s, 3H), 2.83 (br., OH).

2-(Hydroxy(phenyl)methyl)acrylonitrile (5b). The title compound was prepared from the reaction of benzaldehyde with acrylonitrile as a yellowish oil in a yield of 41%. ¹H NMR (300 MHz, CDCl₃): δ 7.43–7.37 (m, 5H), 6.08 (s, 1H), 6.0 (s, 1H), 5.25 (d, J = 4 Hz, 1H), 3.14 (d, J = 4 Hz, 1H).

General Procedure for the Preparation of 6a–b. To the solution of **5a–b** (10 mmol, 1.0 equiv) in anhydrous CH₂Cl₂ (15 mL) was added dropwise PBr₃ (1.42 mL, 15 mmol, 1.5 equiv) at 0 °C. The reaction mixture was allowed to stir at r.t. for 15 min. The mixture was quenched by adding cool water (40 mL) and extracted by CH₂Cl₂ (30 mL × 3). The combined organic solvent was washed by a saturated sodium bicarbonate aqueous solution (30 mL × 3) and brine (30 mL × 3) and dried by anhydrous sodium sulfate. The solvent was concentrated under vacuum and purified by flash chromatography (petroleum ether/EtOAc, 100:1 v/v) to give **6a–b**.

(Z)-Methyl 2-(Bromomethyl)-3-phenylacrylate (6a). The title compound was prepared from the reaction of **5a** with PBr₃ in a yield of 63% as a white solid. ¹H NMR (300 MHz, CDCl₃): δ 7.79 (s, 1H), 7.54 (m, 2H), 7.40 (m, 3H), 4.36 (s, 2H), 3.83 (s, 3H); ¹³C NMR (75 MHz, CDCl₃): δ 166.37, 142.75, 134.24, 129.58, 128.84, 128.80, 52.27, 26.66.

(E/Z)-2-(Bromomethyl)-3-phenylacrylonitrile (6b). The title compound was prepared from the reaction of **5b** with PBr₃ in a yield of 68% as a white solid. **5b** was composed of E and Z isomers, and the ratio was E/Z = 1:3. ¹H NMR (300 MHz, CDCl₃): δ 7.40–7.50 & 7.76–7.84 (m, 5H, aromatic), 7.21 & 7.35 (2s, 1H, olefinic HC=C), 4.19 & 4.22 (2s, 2H, CH₂); ¹³C NMR (75 MHz, CDCl₃): δ 146.52 & 147.20 (HC=C), 132.69 (aromatic), 132.45, 131.36, 130.46, 129.22, 129.05, 118.65 (HC=C & CN), 117.05, 112.05, 108.10, 26.62 & 32.70 (CH₂).

The Synthesis of (E)-(2-Nitrovinyl)benzene (7). To a solution of benzaldehyde (1.06 g, 10.0 mmol, 1.0 equiv) in nitromethane (15 mL) was added ammonium acetate (77 mg, 1.0 mmol, 0.1 equiv). The obtained mixture was heated to 100 °C and stirred for 8 h. The mixture was extracted by EtOAc (30 mL × 3), and the combined organic layers were washed with brine (30 mL × 3) and dried by anhydrous sodium sulfate. The solvent was concentrated under vacuum and purified by flash chromatography (petroleum ether/EtOAc, 10:1 v/v) to give **7** as a yellowish solid in a yield of 85%. ¹H NMR (300 MHz, CDCl₃): δ 8.00 (dd, J = 13.7, 1.8 Hz, 1H), 7.60 (dd, J = 13.7, 1.1 Hz, 1H), 7.52–7.56 (m, 2H), 7.48–7.52 (m, 1H), 7.41–7.48 (m, 2H); ¹³C NMR (75 MHz, CDCl₃): δ 139.23, 137.22, 132.30, 130.17, 129.53, 129.29.

The Synthesis of (E)-2-Nitro-3-phenylprop-2-en-1-ol (8). **7** (119 mg, 0.8 mmol, 1.0 equiv) was dissolved in dry THF (5 mL) and mixed with imidazole (54.4 mg, 0.8 mmol, 1.0 equiv) and

formaldehyde (5 mL). The obtained mixture was allowed to stir at r.t. for 3 days. The reaction was quenched by adding a cool diluted hydrochloric acid solution (20 mL). The mixture was extracted by EtOAc (30 mL \times 3), and the combined organic layers were washed with brine (30 mL \times 3) and dried by anhydrous sodium sulfate. The dry solvent was concentrated under vacuum, and the residue was purified by flash chromatography (petroleum ether/EtOAc, 10:1 v/v) to get **8** as a yellowish oil in a yield of 41%. $^1\text{H NMR}$ (300 MHz, CDCl_3): δ 8.22 (s, 1H), 7.48–7.58 (m, 5H), 4.71 (d, $J = 4.2$ Hz, 2H), 2.61 (s, 1H); $^{13}\text{C NMR}$ (75 MHz, CDCl_3): δ 149.44, 137.67, 131.31, 130.96, 130.19, 129.14, 56.62.

The Synthesis of (E)-(3-Bromo-2-nitroprop-1-en-1-yl)-benzene (9). To the solution of **8** (107 mg, 0.6 mmol, 1.0 equiv) in anhydrous CH_2Cl_2 (15 mL) was added dropwise PBr_3 (0.085 mL, 0.9 mmol, 1.5 equiv) at 0 °C. The reaction mixture was allowed to stir at r.t. for 15 min. The mixture was quenched by adding cool water (40 mL) and extracted by CH_2Cl_2 (30 mL \times 3). The combined organic solvent was washed by a saturated sodium bicarbonate aqueous solution (30 mL \times 3) and brine (30 mL \times 3) and dried by anhydrous sodium sulfate. The dried solvent was concentrated under vacuum, and the residue was purified by flash chromatography (petroleum ether/EtOAc, 20:1 v/v) to give **9** as a yellow solid in a yield of 85%. $^1\text{H NMR}$ (300 MHz, CDCl_3): δ 8.15 (s, 1H), 7.44–7.54 (m, 5H), 4.54 (s, 2H); $^{13}\text{C NMR}$ (75 MHz, CDCl_3): δ 146.85, 137.43, 131.36, 131.20, 130.30, 129.48, 23.26.

General Procedure for the Preparation of 4a–d. To a solution of respective allyl bromide compounds **3**, **6a**, **6b**, or **9** (1 mmol) in 3 mL of ether was added AgNO_2 (183.5 mg, 1.2 mmol). The obtained mixture was stirred overnight at r.t. protected from light. The reaction mixture was filtered, and the filtrate was concentrated under a reduced pressure. The resulting residue was purified by flash chromatography (petroleum ether/EtOAc, 15:1 v/v) to afford the target compounds **4a–d**.

(E)-2-(Nitromethyl)-1,3-diphenylprop-2-en-1-one (4a). The title compound was prepared from intermediate **3** and AgNO_2 as a colorless oil in a yield of 53%. $^1\text{H NMR}$ (300 MHz, CDCl_3): δ 7.88 (d, $J = 7.3$ Hz, 2H), 7.73–7.41 (m, 7H), 7.39–7.28 (m, 2H), 5.60 (s, 2H); $^{13}\text{C NMR}$ (75 MHz, CDCl_3): δ 196.18, 148.43, 137.13, 133.49, 132.79, 130.36, 130.22, 129.88, 129.88, 129.29, 129.03, 128.65, 71.95; ESI-MS (m/z): 290.1 $[\text{M} + \text{Na}]^+$; ESI-HRMS (m/z): calculated for $\text{C}_{16}\text{H}_{13}\text{NNaO}_3$ $[\text{M} + \text{Na}]^+$ 290.0788, found 290.0788.

(E)-Methyl 2-(Nitromethyl)-3-phenylacrylate (4b). The title compound was obtained from **6a** as a colorless oil in a yield of 48%. The NMR data were consistent with a previous report.⁴⁷ $^1\text{H NMR}$ (300 MHz, CDCl_3): δ 8.19 (s, 1H), 7.52–7.40 (m, 3H), 7.36–7.29 (m, 2H), 5.36 (s, 2H), 3.87 (s, 3H).

(Z)-2-(Nitromethyl)-3-phenylacrylonitrile (4c). The title compound was obtained from **6b** as a pale-yellow solid in a yield of 25%. m.p. 99.2–101.2 °C; $^1\text{H NMR}$ (300 MHz, CDCl_3): δ 7.85 (dd, $J = 7.6, 1.4$ Hz, 2H), 7.57–7.42 (m, 3H), 7.32 (s, 1H), 5.18 (s, 2H); $^{13}\text{C NMR}$ (75 MHz, CDCl_3): δ 152.78, 132.45, 131.82, 129.79, 129.32, 116.73, 99.72, 78.31; ESI-MS (m/z): 187.1 $[\text{M} - \text{H}]^-$; ESI-HRMS (m/z): calculated for $\text{C}_{10}\text{H}_7\text{N}_2\text{O}_2$ $[\text{M} - \text{H}]^-$ 187.0513, found 187.0512.

(E)-(2,3-Dinitroprop-1-en-1-yl)benzene (4d). The title compound was obtained from **9**²⁷ as a white solid in a yield of 36%. m.p. 107.6–109.4 °C; $^1\text{H NMR}$ (300 MHz, CDCl_3): δ 8.60 (s, 1H), 7.59–7.40 (m, 5H), 5.65 (s, 2H); $^{13}\text{C NMR}$ (75 MHz, CDCl_3): δ 143.00, 140.01, 132.16, 130.27, 129.78, 129.69, 70.82; ESI-MS (m/z): 290.1 $[\text{M} - \text{NO}_2]^+$; ESI-HRMS (m/z): calculated for $\text{C}_9\text{H}_8\text{NO}_2$ $[\text{M} - \text{NO}_2]^+$ 162.0550, found 162.0558.

Animals. Male SD rats (12 weeks of age, 200–220 g) were obtained from the Shanghai Laboratory Animals Center (SLAC, Shanghai, China) and housed in a specific pathogen-free facility in our campus. The animals were allowed free access to rat chow and water. Additional SD embryos at E18–E19 were obtained from the Experimental Animal Center of Nanjing University, Nanjing, China. All animal experiments and animal care were conducted in accordance with the guidelines and laws of the Provision and General Recommendation of Chinese Experimental Animals in China. The experimental protocols were approved by the Institutional Animal

Care and Use Committee (IACUC) of China Pharmaceutical University (SYXK (SU) 2016-0011).

Measurement of NO_2^- . Analysis of NO_2^- contents *in vitro* was performed by the Griess assay. Briefly, the tested compounds in DMSO were diluted into 50 μM in saline, buffer (various molarities of nucleophiles), or bovine plasma containing 5% DMSO. The samples were incubated at 37 °C for 24 h. Individual samples (50 μL each) were mixed in triplicate with the Griess reagent (150 μL) and incubated at 37 °C for 10 min followed by measurement of the absorbance at 540 nm. The levels of NO_2^- *in vivo* were determined by ion chromatography.²⁴ Briefly, individual male SD rats were injected iv with a single dose of each compound (**4a**: 10 mg/kg or NaNO_2 : 2.44 mg/kg, $N = 3$ per group), and their plasma samples were collected longitudinally. Individual plasma samples (50 μL) were immediately mixed with 2.5 ng of oroxylin A (an internal lane standard, Sigma, St. Louis, USA) in 200 μL of methanol and centrifuged at 20,000g for 10 min. Their supernatants (10 μL each) were used for ion chromatography.

Oxygen–Glucose Deprivation (OGD) and Recovery (R) Induction. Rat cortical neurons were isolated as described previously (<https://www.nature.com/articles/s41598-017-05342-9>). In brief, SD rat embryos at E18–E19 were euthanized by cervical dislocation under general anesthesia. Their brain cortex tissues were dissected out and mechanically cut into small pieces. The brain tissues were enzymatically digested to prepare single cell suspensions. Primary cortical neurons (1×10^6 cells/mL) were cultured onto poly-lysine-coated plates in DMEM supplemented with 10% fetal bovine serum (FBS, Invitrogen, Grand Island, NY) for 4 h at 37 °C in a humidified atmosphere of 95% air and 5% CO_2 to allow cell adhesion. After removal of the unattached cells, the adhered primary cortical neurons were pretreated with **4a** or NaNO_2 (0, 0.9, 11.8, and 3.6 μM) in primary neuron basal medium supplemented with 2% B27 supplement (Invitrogen) for 24 h. After being washed, the cells were cultured in glucose- and FBS-free DMEM in 1% O_2 , 5% CO_2 , and 94% N_2 for 45 min at 37 °C to induce OGD injury. Subsequently, the cells were cultured in 10% FBS DMEM (5% glucose) for 24 h at 37 °C in a humidified atmosphere of 95% air and 5% CO_2 . The cell viability was measured by the MTT assay.

Quantitative Real-Time PCR. Total RNA was extracted from individual groups of primary cortical neurons or brain tissues using the Trizol reagent (Invitrogen) according to the manufacturer's instructions. After determining the quantity and quality, each RNA sample was reversely transcribed into cDNA using a Hiscript II reverse transcriptase kit (Vazyme, Nanjing, China). The relative levels of target gene mRNA transcripts to control GAPDH were determined by RT-qPCR using the SYBR-green mix kit (Hiscript II reverse transcriptase, Vazyme, Nanjing, China) and specific primers (Supporting information Table S1). The data were normalized to GAPDH and analyzed by $2^{-\Delta\Delta\text{Ct}}$.

Western Blotting. The different groups of primary cortical neurons were harvested and their cytoplasmic and nuclear proteins were extracted using the NE-PER nuclear and cytoplasmic extraction kit (Thermo) according to the manufacturer's instruction. The cytoplasmic and nuclear proteins (30 μg /lane) were separated by sodium dodecyl sulfate polyacrylamide gel electrophoresis (SDS-PAGE) on 8–12% gels and transferred onto nitrocellulose (NC) membranes. The membranes were blocked with 5% nonfat dry milk in TBS containing 0.075% Tween-20 (TBST) for 1 h and incubated with primary antibodies (anti-Nrf2, ab137550, 1:1000 dilution; anti-lamin A, ab8980, 1:1000 dilution; and anti- β -actin, ab8227, 1:1000 dilution; Abcam, Cambridge, UK) overnight at 4 °C. After being washed, the bound antibodies were detected with horseradish peroxidase (HRP)-conjugated secondary antibodies for 1 h at room temperature and visualized using the chemiluminescence detection kit (Tanon 6600). The relative levels of target protein expression were determined by densitometric analysis using Image pro plus 6.0 (Media Cybernetics, Silver Spring, USA).

Rat Blood Pressure Measurements. Male SD rats were injected iv with **4a** (950 μg /kg) or the vehicle control through their tail vein ($N = 3$ per group). Their tail artery blood pressures were measured

longitudinally at 0, 1, 2, 3, 4, 5, 6, and 24 h post drug injection using a thermostat noninvasive blood pressure monitor (XH200; Beijing Zhongshi Dichuang Science & Technology Development, Beijing, China).

Drug Treatment and *In Vivo* Anti-IS Evaluation. Male SD rats were randomized and injected iv with the vehicle, sodium nitrite (24.5, 245.4, and 2454 $\mu\text{g}/\text{kg}$), or **4a** (95, 950, and 9500 $\mu\text{g}/\text{kg}$) 2 h before or after ischemia ($N = 8$ per group). One group of rats received sham surgery without MCAO, and another group of rats was injected iv with PTIO (1 mg/kg) 30 min before receiving **4a** treatment.

Subsequently, these rats were injected iv with chloral hydrate (350 mg/kg) and subjected to a procedure of middle cerebral artery occlusion (MCAO).^{48,49} In brief, the MCA of individual rats was exposed and inserted with a 0.30–0.35 mm nylon intraluminal suture to induce MCAO. At 2 h after ischemia, the nylon suture was removed to reperfuse the brain. At 24 h after reperfusion, the neurologic deficits in individual rats were examined by Longa's methods.⁴⁸ The rats were euthanized, and their whole brains were dissected and weighed (wet weight). Their brain sections (2 mm) were stained with triphenyltetrazolium chloride (TTC, Sigma).⁵⁰ The whole brains from some rats in each group were dried in a 105 °C baker for 24 h and weighed (dry weight). The infarction volumes (%) were calculated as infarct area/whole area for each rat. The degrees of brain edema were quantified by the following formula: (wet weight – dry weight)/(wet weight) \times 100 (%).⁵¹

Immunohistochemistry. The levels of NQO-1 and HO-1 expression and Nrf2 phosphorylation in the brain tissues of different groups of rats were analyzed by immunohistochemistry. Briefly, the paraformaldehyde-fixed paraffin-embedded brain tissue sections (3 μm) were deparaffinized, rehydrated, and subjected to antigen retrieval. After being blocked with 10% normal goat sera in PBS, the sections were incubated with rabbit anti-NQO-1 (ab34173, 1:200 dilution), anti-HO-1 (ab13243, 1:200 dilution; Abcam, Cambridge, UK), and anti-phos-Nrf2 (bs-2013R, 1:100 dilution; Beijing Biosynthesis Biotechnology, Beijing, China) at 4 °C overnight, and rabbit IgG from healthy animals served as the negative control. After being washed, the bound antibodies were detected with HRP-conjugated goat anti-rabbit IgG followed by visualizing with diaminobenzidine (DAB; Sigma, St. Louis, MO) and counterstaining with hematoxylin. The staining intensity and the frequency of positively stained cells were scored by the average optical density (AOD) of the positive cells in five fields/sample with the Image-Pro Plus 6.0 software in a blinded manner.

***In Vitro* Tube Formation Assay for the Evaluation of Angiogenesis.** The tube formation experiment was conducted according to a previous report with minor modifications.⁵² Briefly, HUVECs at between two and six generations were cultured in the DMEM with 10% FBS, 2 mM L-glutamine, 1 mM sodium pyruvate, 100 U/mL penicillin, and 100 $\mu\text{g}/\text{mL}$ streptomycin. Matrigel (Cat. No. 356234; Corning, NY, USA) was added to prechilled 96-well plates, and the plates were left in the incubator for 30 min. Then, the HUVEC suspension (at final density of 8×10^4 per well) was added to each well of plates. These HUVECs were incubated with the vehicle or tested compounds, cultured for 8 h at 37 °C and 5% CO₂ atmosphere. The tube formation was observed and counted under an inverted microscope (Ts2R; Nikon, Tokyo, Japan).

***In Vivo* Determination of Angiogenesis.** The different groups of rats ($N = 5$ per group) were treated with the indicated dose of each drug immediately after reperfusion and then daily for 7 consecutive days. The rats were euthanized, and their brain tissues were dissected and fixed. The paraffin-embedded brain tissue sections (3 μm) were subjected to immunohistochemistry using mouse anti-CD31 (ab264089, 1:100; Abcam, Cambridge, UK), as described above. Furthermore, some tissue sections were analyzed by immunofluorescence.^{53,18} Briefly, the brain tissue sections were incubated with anti-CD31 (ab264089, 1:100; Abcam, Cambridge, UK), rabbit anti-Ki67 (ab197547, 1:100; Abcam, Cambridge, UK), or rabbit anti-Aurora (ab45145, 1:100; Abcam, Cambridge, UK) at 4 °C overnight, and after being washed, the bound antibodies were reacted with Cy5-conjugated anti-rabbit IgG (red) and Alexa Fluor 488-conjugated

anti-mouse IgG (green) followed by nuclear staining with DAPI. The fluorescent signals were captured and photo imaged under a fluorescent microscope. Vascular density was calculated by CD31-positive cells divided by DAPI-positive cells. Proliferating vascular cells were measured as the percentages of CD31⁺/Ki67⁺ cells divided by CD31⁺ cells.

Statistical Analysis. Data are expressed as the mean \pm SD. The difference between groups was analyzed by Student's *t* test. The difference in neurologic deficit scores among groups was calculated using the Kruskal–Wallis test and Mann–Whitney *U* test. All the other data were compared using one-way ANOVA and post hoc Tukey's test. All statistical analyses were performed using the SPSS version 20 for Windows. A *P* value of <0.05 was considered statistically significant.

■ ASSOCIATED CONTENT

SI Supporting Information

The Supporting Information is available free of charge at <https://pubs.acs.org/doi/10.1021/acs.jmedchem.1c00282>.

The stability of **4a** in different conditions; reaction kinetics of **4a** and GSH; the pharmacokinetic behavior of **4a** (including concentration–time curve and calculated pharmacokinetic parameters); the effects of **4a** on enhancing Nrf2 signaling and activating the sGC/cGMP/PKG pathway in OGD/R rat primary cortical neurons, on blood pressure in rats, on enhancing the Nrf2 pathway in MCAO rats, and on the angiogenesis *in vitro*; the primers used in the real-time quantitative PCR; the HPLC analytical parameters of plasma NO₂⁻ levels and a representative chromatogram; HRMS spectra of the intermediates formed by the reaction of **4a** with thiols; the ¹H NMR, ¹³C NMR, and HRMS spectra for compounds **4a**, **4c**, and **4d**; and the HPLC traces for the purity of compounds **4a–d** (PDF)

Molecular formula strings for compounds **4a–d** (CSV)

■ AUTHOR INFORMATION

Corresponding Authors

Zhangjian Huang – State Key Laboratory of Natural Medicines, Jiangsu Key Laboratory of Drug Discovery for Metabolic Diseases, Jiangsu Key Laboratory of Drug Screening, China Pharmaceutical University, Nanjing 210009, P.R. China; orcid.org/0000-0001-6409-8535; Phone: +86-25-83271072; Email: zhangjianhuang@cpu.edu.cn; Fax: +86-25-83271072

Xiaojun Xu – State Key Laboratory of Natural Medicines, Jiangsu Key Laboratory of Drug Discovery for Metabolic Diseases, Jiangsu Key Laboratory of Drug Screening, China Pharmaceutical University, Nanjing 210009, P.R. China; Phone: +86 18066069538; Email: xiaojunxu2000@163.com

Yihua Zhang – State Key Laboratory of Natural Medicines, Jiangsu Key Laboratory of Drug Discovery for Metabolic Diseases, Jiangsu Key Laboratory of Drug Screening, China Pharmaceutical University, Nanjing 210009, P.R. China; orcid.org/0000-0003-2378-7064; Phone: +86-25-83271015; Email: zyhtgd@163.com; Fax: +86-25-83271015

Authors

Jianbing Wu – State Key Laboratory of Natural Medicines, Jiangsu Key Laboratory of Drug Discovery for Metabolic Diseases, Jiangsu Key Laboratory of Drug Screening, China

Pharmaceutical University, Nanjing 210009, P.R. China;

orcid.org/0000-0003-2725-9859

Wei Yin – State Key Laboratory of Natural Medicines, Jiangsu Key Laboratory of Drug Discovery for Metabolic Diseases, Jiangsu Key Laboratory of Drug Screening, China

Pharmaceutical University, Nanjing 210009, P.R. China

Yinqiu Zhang – State Key Laboratory of Natural Medicines, Jiangsu Key Laboratory of Drug Discovery for Metabolic Diseases, Jiangsu Key Laboratory of Drug Screening, China

Pharmaceutical University, Nanjing 210009, P.R. China

Jian Jia – State Key Laboratory of Natural Medicines, Jiangsu Key Laboratory of Drug Discovery for Metabolic Diseases, Jiangsu Key Laboratory of Drug Screening, China

Pharmaceutical University, Nanjing 210009, P.R. China

Huimin Cheng – State Key Laboratory of Natural Medicines, Jiangsu Key Laboratory of Drug Discovery for Metabolic Diseases, Jiangsu Key Laboratory of Drug Screening, China

Pharmaceutical University, Nanjing 210009, P.R. China

Fenghua Kang – State Key Laboratory of Natural Medicines, Jiangsu Key Laboratory of Drug Discovery for Metabolic Diseases, Jiangsu Key Laboratory of Drug Screening, China

Pharmaceutical University, Nanjing 210009, P.R. China

Kai Huang – The Department of Cardiology, Institute of Cardiovascular Disease, Union Hospital, Tongji Medical College, Huazhong University of Science and Technology, Wuhan 430074, P.R. China

Tao Sun – State Key Laboratory of Natural Medicines, Jiangsu Key Laboratory of Drug Discovery for Metabolic Diseases, Jiangsu Key Laboratory of Drug Screening, China

Pharmaceutical University, Nanjing 210009, P.R. China

Jide Tian – Department of Molecular and Medical Pharmacology, University of California, Los Angeles, California 90095, United States

Complete contact information is available at:

<https://pubs.acs.org/10.1021/acs.jmedchem.1c00282>

Author Contributions

#J.W. and W.Y. contributed equally to this work. J.W. and W.Y. designed and synthesized compounds, carried out the experiments, and analyzed data. F.K., K.H., and T.S. performed biochemical assays. J.J. conducted HPLC determination. H.C. performed the *in vitro* angiogenesis assay. Z.H., X.X., and Y.Z. supervised the research. J.W., W.Y., Z.H., J.T., X.X., and Y.Z. wrote the manuscript. Y.Z. conceived the project. Biological assays: Nanjing Biorn Lifescience (abbreviated as *Biorn*) conducted biological assays.

Notes

The authors declare no competing financial interest.

ACKNOWLEDGMENTS

We gratefully acknowledge the National Natural Science Foundation of China (Nos. 81773573, 21372261, 81673305, and 81273378); Jiangsu Province Funds for Distinguished Young Scientists (BK20160033) and the 111 Project (B16046); the Open Project Program of State Key Laboratory of Natural Medicines, China Pharmaceutical University (SKLNMZZCX201820); and the "Double First-Class" University Project (CPU2018GF04) for the financial support.

ABBREVIATIONS

AIS, acute ischemic stroke; AOD, average optical density; ARE, antioxidant response element; cGMP, cyclic guanosine

monophosphate; Cys, cysteine; DAB, diaminobenzidine; DABCO, 1,4-diaza[2.2.2]bicyclooctane; deoxy-Hb, deoxygenated hemoglobin; ESI, electrospray ionization; FBS, fetal bovine serum; FDA, Food and Drug Administration; GAPDH, reduced glyceraldehyde-phosphate dehydrogenase; GSH, glutathione; HO, hemeoxygenase-1; HPLC, high-performance liquid chromatography; HRMS, high-resolution mass spectrometry; HRP, horseradish peroxidase; HUVECs, human umbilical vein endothelial cells; IHC, immunohistochemistry; IS, ischemic stroke; I/R, ischemia/reperfusion; IQR, interquartile range; Keap1, Kelch-like ECH-associated protein 1; LDH, lactate dehydrogenase; MCA, middle cerebral artery; MCAO, middle cerebral artery occlusion; MTT, methyl thiazolyl tetrazolium; NaNO₂, sodium nitrite; NC, nitrocellulose; NO, nitric oxide; NO₂⁻, nitrite; NO₃⁻, nitrate; NQO-1, NADPH quinoneoxidoreductase-1; Nrf2, nuclear factor (erythroid-derived 2)-like 2; OGD/R, oxygen–glucose deprivation/recovery; PKG, protein kinase G; Pro, proline; PTIO, 2-phenyl-4,4,5,5-tetramethylimidazole-1-oxyl 3-oxide; RT-qPCR, reverse transcription-quantitative polymerase chain reaction; sGC, soluble guanylate cyclase; SD, Sprague–Dawley; SDS-PAGE, sodium dodecyl sulfate polyacrylamide gel electrophoresis; TBHQ, *tert*-butylhydroquinone; TBST, TBS containing 0.075% Tween-20; TTC, triphenyltetrazolium chloride; tPA, tissue plasminogen activator; *t*_{1/2}, half-life period; XOR, xanthine oxidoreductase

REFERENCES

- (1) Saver, J. L.; Starkman, S.; Eckstein, M.; Stratton, S. J.; Pratt, F. D.; Hamilton, S.; Conwit, R.; Liebeskind, D. S.; Sung, G.; Kramer, I.; Moreau, G.; Goldweber, R.; Sanossian, N.; FAST-MAG Investigators and Coordinators. Prehospital use of magnesium sulfate as neuroprotection in acute stroke. *N. Engl. J. Med.* **2015**, *372*, 528–536.
- (2) Chamorro, A.; Dirnagl, U.; Urra, X.; Planas, A. M. Neuroprotection in acute stroke: Targeting excitotoxicity, oxidative and nitrosative stress, and inflammation. *Lancet Neurol.* **2016**, *15*, 869–881.
- (3) Saver, J. L.; Goyal, M.; Bonafe, A.; Diener, H.-C.; Levy, E. I.; Pereira, V. M.; Albers, G. W.; Cognard, C.; Cohen, D. J.; Hacke, W.; Jansen, O.; Jovin, T. G.; Mattle, H. P.; Nogueira, R. G.; Siddiqui, A. H.; Yavagal, D. R.; Baxter, B. W.; Devlin, T. G.; Lopes, D. K.; Reddy, V. K.; du Mesnil de Rochemont, R.; Singer, O. C.; Jahan, R. Stent-retriever thrombectomy after intravenous t-PA vs. t-PA alone in stroke. *N. Engl. J. Med.* **2015**, *372*, 2285–2295.
- (4) Lo, E. H. A new penumbra: Transitioning from injury into repair after stroke. *Nat. Med.* **2008**, *14*, 497–500.
- (5) Krupinski, J.; Kaluza, J.; Kumar, P.; Kumar, S.; Wang, J. M. Role of angiogenesis in patients with cerebral ischemic stroke. *Stroke* **1994**, *25*, 1794–1798.
- (6) Shiva, S.; Sack, M. N.; Greer, J. J.; Duranski, M.; Ringwood, L. A.; Burwell, L.; Wang, X.; MacArthur, P. H.; Shoja, A.; Raghavachari, N.; Calvert, J. W.; Brookes, P. S.; Lefer, D. J.; Gladwin, M. T. Nitrite augments tolerance to ischemia/reperfusion injury via the modulation of mitochondrial electron transfer. *J. Exp. Med.* **2007**, *204*, 2089–2102.
- (7) Wink, D. A.; Hanbauer, I.; Krishna, M. C.; DeGraff, W.; Gamson, J.; Mitchell, J. B. Nitric oxide protects against cellular damage and cytotoxicity from reactive oxygen species. *Proc. Natl. Acad. Sci. U. S. A.* **1993**, *90*, 9813–9817.
- (8) Stuehr, D.; Pou, S.; Rosen, G. M. Oxygen reduction by nitric-oxide synthases. *J. Biol. Chem.* **2001**, *276*, 14533–14536.
- (9) Pluta, R. M.; Rak, R.; Wink, D. A.; Woodward, J. J.; Khaldi, A.; Oldfield, E. H.; Watson, J. C. Effects of nitric oxide on reactive oxygen species production and infarction size after brain reperfusion injury. *Neurosurgery* **2001**, *48*, 884–893. discussion 892–893

- (10) Ignarro, L. J.; Napoli, C.; Loscalzo, J. Nitric oxide donors and cardiovascular agents modulating the bioactivity of nitric oxide: An overview. *Circ. Res.* **2002**, *90*, 21–28.
- (11) Zhang, R.; Wang, L.; Zhang, L.; Chen, J.; Zhu, Z.; Zhang, Z.; Chopp, M. Nitric oxide enhances angiogenesis via the synthesis of vascular endothelial growth factor and cGMP after stroke in the rat. *Circ. Res.* **2003**, *92*, 308–313.
- (12) Schopfer, F. J.; Baker, P. R. S.; Freeman, B. A. NO-dependent protein nitration: A cell signaling event or an oxidative inflammatory response? *Trends Biochem. Sci.* **2003**, *28*, 646–654.
- (13) Lundberg, J. O.; Weitzberg, E.; Lundberg, J. M.; Alving, K. Intragastric nitric oxide production in humans: Measurements in expelled air. *Gut* **1994**, *35*, 1543–1546.
- (14) Zweier, J. L.; Wang, P.; Samouilov, A.; Kuppusamy, P. Enzyme-independent formation of nitric oxide in biological tissues. *Nat. Med.* **1995**, *1*, 804–809.
- (15) Cosby, K.; Partovi, K. S.; Crawford, J. H.; Patel, R. P.; Reiter, C. D.; Martyr, S.; Yang, B. K.; Waclawiw, M. A.; Zalos, G.; Xu, X.; Huang, K. T.; Shields, H.; Kim-Shapiro, D. B.; Schechter, A. N.; Cannon, R. O., III; Gladwin, M. T. Nitrite reduction to nitric oxide by deoxyhemoglobin vasodilates the human circulation. *Nat. Med.* **2003**, *9*, 1498–1505.
- (16) Omar, S. A.; Webb, A. J. Nitrite reduction and cardiovascular protection. *J. Mol. Cell. Cardiol.* **2014**, *73*, 57–69.
- (17) Lundberg, J. O.; Weitzberg, E.; Gladwin, M. T. The nitrate-nitrite-nitric oxide pathway in physiology and therapeutics. *Nat. Rev. Drug Discovery* **2008**, *7*, 156–167.
- (18) Kumar, D.; Branch, B. G.; Pattillo, C. B.; Hood, J.; Thoma, S.; Simpson, S.; Illum, S.; Arora, N.; Chidlow, J. H.; Langston, W.; Teng, X.; Lefer, D. J.; Patel, R. P.; Kevil, C. G. Chronic sodium nitrite therapy augments ischemia-induced angiogenesis and arteriogenesis. *Proc. Natl. Acad. Sci. U. S. A.* **2008**, *105*, 7540–7545.
- (19) Pluta, R. M.; Oldfield, E. H.; Bakhtian, K. D.; Fathi, A. R.; Smith, R. K.; Devroom, H. L.; Nahavandi, M.; Woo, S.; Figg, W. D.; Lonser, R. R. Safety and feasibility of long-term intravenous sodium nitrite infusion in healthy volunteers. *PLoS One* **2011**, *6*, No. e14504.
- (20) Duranski, M. R.; Greer, J. J. M.; Dejam, A.; Jaganmohan, S.; Hogg, N.; Langston, W.; Patel, R. P.; Yet, S.-F.; Wang, X.; Kevil, C. G.; Gladwin, M. T.; Lefer, D. J. Cytoprotective effects of nitrite during *in vivo* ischemia-reperfusion of the heart and liver. *J. Clin. Invest.* **2005**, *115*, 1232–1240.
- (21) Liu, M.; Zollbrecht, C.; Peleli, M.; Lundberg, J. O.; Weitzberg, E.; Carlström, M. Nitrite-mediated renal vasodilatation is increased during ischemic conditions via cGMP-independent signaling. *Free Radical Biol. Med.* **2015**, *84*, 154–160.
- (22) Jung, K.-H.; Chu, K.; Ko, S.-Y.; Lee, S.-T.; Sinn, D.-I.; Park, D.-K.; Kim, J.-M.; Song, E.-C.; Kim, M.; Roh, J.-K. Early intravenous infusion of sodium nitrite protects brain against *in vivo* ischemia-reperfusion injury. *Stroke* **2006**, *37*, 2744–2750.
- (23) Chakrapani, H.; Gorczynski, M. J.; King, S. B. Allylic nitro compounds as nitrite donors. *J. Am. Chem. Soc.* **2006**, *128*, 16332–16337.
- (24) Rassaf, T.; Bryan, N. S.; Kelm, M.; Feelisch, M. Concomitant presence of n-nitroso and s-nitroso proteins in human plasma. *Free Radical Biol. Med.* **2002**, *33*, 1590–1596.
- (25) Kumar, V.; Kumar, S.; Hassan, M.; Wu, H.; Thimmulappa, R. K.; Kumar, A.; Sharma, S. K.; Parmar, V. S.; Biswal, S.; Malhotra, S. V. Novel chalcone derivatives as potent Nrf2 activators in mice and human lung epithelial cells. *J. Med. Chem.* **2011**, *54*, 4147–4159.
- (26) Liu, L.; Locascio, L. M.; Dore, S. Critical role of Nrf2 in experimental ischemic stroke. *Front. Pharmacol.* **2019**, *10*, 153.
- (27) Bakthadoss, M.; Sivakumar, N.; Devaraj, A.; Kumar, P. V. Synthesis of highly diversified 1,2,3-triazole derivatives via domino [3 + 2] azide cycloaddition and denitration reaction sequence. *RSC Adv.* **2015**, *5*, 93447–93451.
- (28) Zhuang, C.; Zhang, W.; Sheng, C.; Zhang, W.; Xing, C.; Miao, Z. Chalcone: A privileged structure in medicinal chemistry. *Chem. Rev.* **2017**, *117*, 7762–7810.
- (29) Liu, X.; Zhu, Q.; Zhang, M.; Yin, T.; Xu, R.; Xiao, W.; Wu, J.; Deng, B.; Gao, X.; Gong, W.; Lu, G.; Ding, Y. Isoliquiritigenin ameliorates acute pancreatitis in mice via inhibition of oxidative stress and modulation of the Nrf2/HO-1 pathway. *Oxid. Med. Cell. Longevity* **2018**, *2018*, 7161592.
- (30) Qiu, Y.-B.; Wan, B.-B.; Liu, G.; Wu, Y.-X.; Chen, D.; Lu, M.-D.; Chen, J.-L.; Yu, R.-Q.; Chen, D.-Z.; Pang, Q.-F. Nrf2 protects against seawater drowning-induced acute lung injury via inhibiting ferroptosis. *Respir. Res.* **2020**, *21*, 232.
- (31) Greenberg, D. Angiogenesis and stroke. *Drug News Perspect.* **1998**, *11*, 265–270.
- (32) Shanab, A. Y.; Elshaer, S. L.; El-Azab, M. F.; Soliman, S.; Sabbineni, H.; Matragoon, S.; Fagan, S. C.; El-Remessy, A. B. Candesartan stimulates reparative angiogenesis in ischemic retinopathy model: Role of hemeoxygenase-1 (HO-1). *Angiogenesis* **2015**, *18*, 137–150.
- (33) Kim, J.-H.; Lee, K.-S.; Lee, D.-K.; Kim, J.; Kwak, S.-N.; Ha, K.-S.; Choe, J.; Won, M.-H.; Cho, B.-R.; Jeoung, D.; Lee, H.; Kwon, Y.-G.; Kim, Y.-M. Hypoxia-responsive microRNA-101 promotes angiogenesis via heme oxygenase-1/vascular endothelial growth factor axis by targeting cullin 3. *Antioxid. Redox Signaling* **2014**, *21*, 2469–2482.
- (34) Kuang, L.; Feng, J.; He, G.; Jing, T. Knockdown of Nrf2 inhibits the angiogenesis of rat cardiac micro-vascular endothelial cells under hypoxic conditions. *Int. J. Biol. Sci.* **2013**, *9*, 656–665.
- (35) Mazzone, M.; Carmeliet, P. Drug discovery: A lifeline for suffocating tissues. *Nature* **2008**, *453*, 1194–1195.
- (36) Godber, B. L. J.; Doel, J. J.; Sapkota, G. P.; Blake, D. R.; Stevens, C. R.; Eisenthal, R.; Harrison, R. Reduction of nitrite to nitric oxide catalyzed by xanthine oxidoreductase. *J. Biol. Chem.* **2000**, *275*, 7757–7763.
- (37) Nishino, T.; Okamoto, K.; Eger, B. T.; Pai, E. F.; Nishino, T. Mammalian xanthine oxidoreductase- mechanism of transition from xanthine dehydrogenase to xanthine oxidase. *FEBS J.* **2008**, *275*, 3278–3289.
- (38) Wei, L.; Mackenzie, I. S.; MacDonald, T. M.; George, J. Cardiovascular risk associated with sodium-containing medicines. *Expert Opin. Drug Saf.* **2014**, *13*, 1515–1523.
- (39) Kim, K. H.; Kim, S. H.; Lee, H. J.; Kim, J. N. Palladium-catalyzed domino cyclization (5-exo/3-exo), ring-expansion by palladium rearrangement, and aromatization: An expedient synthesis of 4-arylnicotinates from morita-baylis-hillman adducts. *Adv. Synth. Catal.* **2013**, *355*, 1977–1983.
- (40) Basavaiah, D.; Reddy, K. R.; Kumaragurubaran, N. An expedient, facile and simple one-pot synthesis of 2-methylenealkanoates and alkanenitriles from the baylis-hillman bromides in aqueous media. *Nat. Protoc.* **2007**, *2*, 2665–2676.
- (41) Auvray, P.; Knochel, P.; Normant, J. F. Preparation and nucleophilic substitution of (E)-1-bromo-2-phenylsulfonyl-2-alkenes and 3-acetoxy-2-phenylsulfonyl-1-alkenes. *Tetrahedron* **1988**, *44*, 6095–6106.
- (42) Xia, X.-F.; Shu, X.-Z.; Ji, K.-G.; Yang, Y.-F.; Shaikat, A.; Liu, X.-Y.; Liang, Y.-M. Platinum-catalyzed michael addition and cyclization of tertiary amines with nitroolefins by dehydrogenation of α,β -sp³ C-H bonds. *J. Org. Chem.* **2010**, *75*, 2893–2902.
- (43) Cao, C.-L.; Zhou, Y.-Y.; Zhou, J.; Sun, X.-L.; Tang, Y.; Li, Y.-X.; Li, G.-Y.; Sun, J. An organocatalytic asymmetric tandem reaction for the construction of bicyclic skeletons. *Chem. – Eur. J.* **2009**, *15*, 11384–11389.
- (44) Bakthadoss, M.; Sivakumar, N.; Devaraj, A. First synthesis of bromo and chloro derivatives of baylis-hillman adducts derived from nitroolefins: Application towards the synthesis of a dendrimer core. *Synthesis* **2011**, *2011*, 611–618.
- (45) Wei, Y.; Tang, J.; Cong, X.; Zeng, X. Practical metal-free synthesis of chalcone derivatives via a tandem cross-dehydrogenative-coupling/elimination reaction. *Green Chem.* **2013**, *15*, 3165–3169.
- (46) Rebman, R.; Cromwell, N. H. P.; Cromwell, N. H. Mobile keto allyl systems. I. Rearrangements in the synthesis of α -[(n-t-butylamino)-methyl]-chalcone. *Tetrahedron Lett.* **1965**, *6*, 4833–4836.

(47) Hong, W. P.; Lee, K.-J. Synthesis of methyl (*E*)-2-nitromethylcinnamates derived from baylis-hillman acetates and conversion into several coumarin derivatives. *Synthesis* **2005**, *2005*, 33–38.

(48) Longa, E. Z.; Weinstein, P. R.; Carlson, S.; Cummins, R. Reversible middle cerebral artery occlusion without craniectomy in rats. *Stroke* **1989**, *20*, 84–91.

(49) Gerriets, T.; Li, F.; Silva, M. D.; Meng, X.; Brevard, M.; Sotak, C. H.; Fisher, M. The macrosphere model: Evaluation of a new stroke model for permanent middle cerebral artery occlusion in rats. *J. Neurosci. Methods* **2003**, *122*, 201–211.

(50) Sasaki, M.; Honmou, O.; Kocsis, J. D. *A rat middle cerebral artery occlusion model and intravenous cellular delivery*; Humana Press: Totowa, NJ, 2009, pp. 187–195.

(51) Jung, K.-H.; Chu, K.; Jeong, S.-W.; Han, S.-Y.; Lee, S.-T.; Kim, J.-Y.; Kim, M.; Roh, J.-K. Hmg-CoA reductase inhibitor, atorvastatin, promotes sensorimotor recovery, suppressing acute inflammatory reaction after experimental intracerebral hemorrhage. *Stroke* **2004**, *35*, 1744–1749.

(52) Jiang, T.; Shen, S.; Wang, T.; Li, M.; He, B.; Mo, R. A substrate-selective enzyme-catalysis assembly strategy for oligopeptide hydrogel-assisted combinatorial protein delivery. *Nano Lett.* **2017**, *17*, 7447–7454.

(53) Senthilkumar, A.; Smith, R. D.; Khitha, J.; Arora, N.; Veerareddy, S.; Langston, W.; Chidlow, J. H., Jr.; Barlow, S. C.; Teng, X.; Patel, R. P.; Lefter, D. J.; Kevil, C. G. Sildenafil promotes ischemia-induced angiogenesis through a PKG-dependent pathway. *Arterioscler., Thromb., Vasc. Biol.* **2007**, *27*, 1947–1954.